# 4th SFERA-III* / 17th SOLLAB
# Doctoral Colloquium 2023

**September 11th – 13th 2023**

**DLR, Cologne, Germany**



# Book of Abstracts

# Doctoral Colloquium

**September 11th – 13th 2023**
**Location: DLR Casino**

**Monday, September 11th**

| | |
|---|---|
| 8:30 – 9:00 | *Registration* |
| | at the entrance to DLR Casino |
| 9:00 – 9:10 | *Opening and Welcome* |
| | by Prof. Robert Pitz-Paal, DLR |

| | **Session 1: Solar Systems** |
|---|---|
| | Chair: Prof. Manuel Romero, IMDEA |
| 9:10 – 9:30 | **Hybridization of Concentrated Solar Power with Geothermal and Biomass Power** |
| | Bertuğ Çelebi, METU |
| 9:30 – 9:50 | **Comparison of Conventional and Microwave Heating of Solar Salt** |
| | Cristóbal Valverde, CIEMAT |
| 9:50 – 10:10 | **Competitiveness of Carnot Batteries in power generation and industrial applications** |
| | Tiago R. Eusébio, EVORA |
| 10:10 – 10:30 | **Developing a Digital Twin of the Solar Field of Solar Tower Plants** |
| | Maitane Ferreres Eceiza, Fraunhofer ISE |

| | |
|---|---|
| 10:30 – 11:00 | *Coffee Break* |

| | |
|---|---|
| 11:00 – 11:20 | **Application of AI methods to improve Operation and maintenance of CSP power plants** |
| | Thomas Kraft, Fraunhofer ISE |
| 11:20 – 11:40 | **Condition Monitoring for Heliostat Fields using Artificial Intelligence** |
| | Dominik Steinberg, DLR |
| 11:40 – 12:00 | **IoT and Big Data platforms as the basis for autonomous complex systems in Industry 4.0** |
| | Inga Miadowicz, DLR |

| | |
|---|---|
| 12:00 – 13:30 | *Lunch* |

| | |
|---|---|
| | **Session 2: Solar Optics** |
| | Chair: Prof. Alain Dollet, PROMES |
| 13:30 – 13:50 | **Simulation Environment for Developing and Testing UAV-Based CSP Condition Monitoring Systems** |
| | Alexander Schnerring, DLR |
| 13:50 – 14:10 | **Using Synthetic Data for Developing Deep Learning Based Airborne Monitoring Methods for Solar Tower Power Plants** |
| | Rafal Broda, DLR |
| 14:10 – 14:30 | **Characterization and Optimization of High Reflectivity Mirrors for Solar Towers** |
| | Eslem Enis Atak, METU |
| 14:30 – 15:00 | *Coffee Break* |
| 15:00 – 15:20 | **Spectral analysis and ray tracing of Fresnel solar furnace model (PSA) using OTSun software** |
| | Noelia Estremera-Pedriza, CIEMAT |
| 15:20 – 15:40 | **Development of Switchable Technology for Agrivoltaic** |
| | Rebecca Cizek, DLR |
| | **Session 3: Solar Water Treatment** |
| | Chair: Prof. Sixto Malato, CIEMAT |
| 15:40 – 16:00 | **Towards the optimal coupling of multi-effect distillation with solar energy** |
| | Juan Miguel Serrano, CIEMAT |
| 16:00 – 16:30 | *Coffee Break* |
| 16:30 – 16:50 | **ASSESSMENT OF TWO SOLAR PHOTOREACTOR´S DESIGN FOR WATER DECONTAMINATION USING PHOTO FENTON REACTIONS.** |
| | Kelly J. Castañeda Retavizca, CIEMAT |
| 16:50 – 17:10 | **A competitive sustainable solution to treat WWTP secondary effluent for reusing in agriculture: chlor-photo-Fenton** |
| | Solaima Belachqer-El Attar, CIEMAT |
| 17:10 – 17:30 | **Design and simulation of a model-based control system for the automated operation of the solar photo-Fenton process** |
| | Daniel Rodríguez-García, CIEMAT |
| 18:00 | ***Dinner at Eltzhof*** |

# Doctoral Colloquium

## September 11th – 13th 2023
## Location: DLR Casino

**Tuesday, September 12th**

| | |
|---|---|
| | **Session 4: Solar Fuels and Materials** |
| | Chairs: Prof. Christian Sattler and Dr. Stefan Brendelberger, DLR |
| 9:00 – 9:20 | **Thermochemical oxygen pumps: A promising candidate to increase the efficiency of thermochemical fuel production** |
| | Jens Keller, DLR |
| 9:20 – 9:40 | **Hydrogen production improvements by glycerol photoreforming under natural radiation at pilot scale** |
| | Joyce G. Villachica Llamosas, CIEMAT |
| 9:40 – 10:00 | **Development of a thermally coupled photoelectrochemical system for water splitting under concentrated sunlight** |
| | Elisa Gruber, DLR |
| 10:00 – 10:20 | **Development and Investigation of a Reactive Heat Exchanger** |
| | Anika Weber, DLR |
| 10:20 – 11:00 | *Coffee Break* |
| 11:00 – 11:20 | **Modeling the $CeO_2$-$CH_4$-$CO_2$ Redox Reforming Cycle in OpenFOAM** |
| | Mario Zuber, ETH Zurich |
| 11:20 – 11:40 | **3D-Printed Ceria Structures for Enhanced Radiative Heat Transfer of Concentrated Solar Energy** |
| | Sebastian Sas Brunser, ETH Zurich |
| 11:40 – 12:00 | **Development of a Redox Material Assembly for Solar Thermochemical Fuel Production** |
| | Louis Thomas, DLR |
| 12:00 – 13:30 | *Lunch* |
| 13:30 – 13:50 | **Concentrating solar thermal synthesis of $C12A7:e^-$ electrides, a photothermal catalyst for solar fuels production** |
| | Ehsan, Hajialilou, IMDEA |
| 13:50 – 14:10 | **Thermogravimetric study of Sr- and Al-based metal nitrides for the thermochemical production of ammonia** |
| | Daniel Notter, ETH Zurich |
| 14:30 | Social activity |

# Doctoral Colloquium

**September 11th – 13th 2023**
**Location: DLR Casino**

**Wednesday, September 13th**

| | |
|---|---|
| | **Session 5: Solar Receivers** |
| | Chair: Prof. Aldo Steinfeld, ETH Zurich |
| 9:30 – 9:50 | **Development of a High-Temperature Counter-Flow Particle Receiver for Concentrated Solar Power Applications** |
| | Anton Hartner, ETH Zurich |
| 9:50 – 10:10 | **Evaluation of the efficiency and pressure drop in metallic wire meshes with stagger pattern for solar tower technology** |
| | Daniel Sanchez-Señoran, CIEMAT |
| 10:10 – 10:30 | **Development of a nanofluid-based direct absorption parabolic trough solar collector using carbon nanoparticles** |
| | Miguel Sainz Manas, PROMES |
| 10:30 – 11:00 | *Coffee Break* |
| 11:00 – 11:20 | **Numerical investigation of a directly irradiated solar rotary kiln for limestone calcination to maximize $CO_2$ flow and purity** |
| | Jana Barabas, DLR |
| 11:20 – 11:40 | **High temperature aging of fluoro- and perfluororubber: Application in a receiver-reactor cavity system** |
| | Estefanía Vega Puga, DLR |
| 11:40 – 12:00 | **Progress in modelling the thermal performance of a Linear Fresnel Collector with a Trapezoidal Cavity Multi-tube Receiver** |
| | Sergio Alcalde-Morales, CIEMAT |
| 12:00 – 14:00 | *Lunch and Break* |
| 14:00 – 19:00 | **Technical Visit to Solar Tower Jülich** |

# Hybridization of Concentrated Solar Power with Geothermal and Biomass Power

Bertuğ Çelebi[1], Shahab Rohani[2], and Derek Baker[3]
[1]MSc. Student; [3]Professor; Dept. of Mechanical Engineering, Middle East Technical University, Ankara, Turkiye
[2]Scientific Researcher at Fraunhofer Institute for Solar Energy Systems. Heidenhofstr. 2, 79110, Freiburg, Germany
bertug.celebi@metu.edu.tr

## 1. Introduction

CSP without TES produces variable electricity throughout the day, the maximum daily output occurs in the summer. Geothermal power plants (GPPs) offer continuous power production through the year, but the output can decrease significantly during the summer due to high condenser temperatures. Biomass offers continuous and flexible power production through the day, but some biomass sources vary with season. Also, many GPPs have excess capacities due to underperforming geothermal fields [1]. So, hybridizing these technologies potentially offer flexible and dispatchable power while exploiting excess GPP power capacity.

Turkiye, the largest geothermal potential in Europe and fourth largest in the world. All GPPs in Turkiye are based in Aegean Region [2]. Turkiye's Aegean receives high solar irradiance [3] and has a large agricultural sector that produces a variety of biomass resources as waste.

This study is based on the Kızıldere-II (KZD2) GPP, a triple flash and binary hybrid GPP with excess power block capacity located in Denizli in Turkiye's Aegean region. The average annual DNI for Denizli is 1800 – 2000 kWh/m$^2$ [3]. One of the main biomass sources in Denizli is olive residue, which has a high calorific value and is abundant in winter when solar resources tend to be smaller [1]. This site is a good candidate for a hybrid plant.

## 2. Methodology

A simplified diagram of the hybrid plant is in Figure 1. The topping cycle is a steam Rankine cycle run by CSP-biomass combining parabolic trough collectors (PTCs) with biomass combustion (BC) using the local olive residue. The topping cycle's waste heat and heat from BC are used to turn the GPP condensate water from the wet cooling tower (WCT) into steam. This steam is added to the intermediate pressure turbine (IPT) of GPP. The KZD2 GPP has three turbines HPT, IPT, and LPT. The HPT exit is used in the binary part of KZD2.

Also, the HPT has a higher non-condensable gas percentage than IPT, 16.7 % to 0.40 % by weight [2], harmful to energetic performance. The IPT was chosen. Overall, it is desired to increase the power output and make the system more dispatchable, and meet daily and seasonal demands by utilizing the flexibility of the resources.



CST (PTC) System: Converts the topping cycle's feedwater into superheated steam.

1st Loop: Topping CSP-Biomass Rankine Cycle: Both PTC and BC generate steam at same pressure, subsequently two steam flows are mixed and expanded through a turbine, generating power.

2nd Loop: Bottoming Cycle using IPT of GPP: Condensed water from WCT is heated and turned into steam by topping cycle waste heat and BC, respectively. Utilizing excess IPT capacity.

Figure 1. Simplified Diagram of the Hybrid Plant

## 3. Results

The modeling is carried out in TRNSYS Version 18.05.0001 with TESS Libraries Version 17.2.01. The excess power block capacity in IPT is taken 20%, [1, 2]. The PTC is modeled for N-S orientation and E-W single-axis tracking, accounting shading losses. Therminol VP-1 oil is used as the heat transfer fluid with temperature-dependent properties [4]. Mass flow is 35 kg/s, the collectors are of 1.8 m focal length, 47 m length of a single SCA with 8 SCAs in series, and 24 rows of PTCs. For the topping cycle, a steam turbine of 20 MW rated capacity is used with 70 % isentropic efficiency. The biomass burner utilizes olive residue and operates constantly, producing steam at 10 bar and 370 °C. Then mixing with the steam produced by the PTC and expanding in the turbine. Lastly, the waste heat from the turbine exit and heat from BC heat the GPP condensate to the inlet conditions of IPT, 3.5 bar, and 139 °C [2]. Simulations are for a one-week period in August using local weather data and a time step of 0.1 hr. The results are presented in Figure 2, and it can be seen in sunny and clear sky, more than 19 MW$_e$ power can be get, and excess IPT capacity of 20% is used.

## 4. Conclusion

These analyses demonstrate that the hybridization of CSP-biomass-geothermal can potentially exploit the excess power block capacity of a GPP in Denizli, Turkiye, and provide additional power during hours with high solar irradiance, and if desired biomass combustion can be adjusted to enable flexible production.
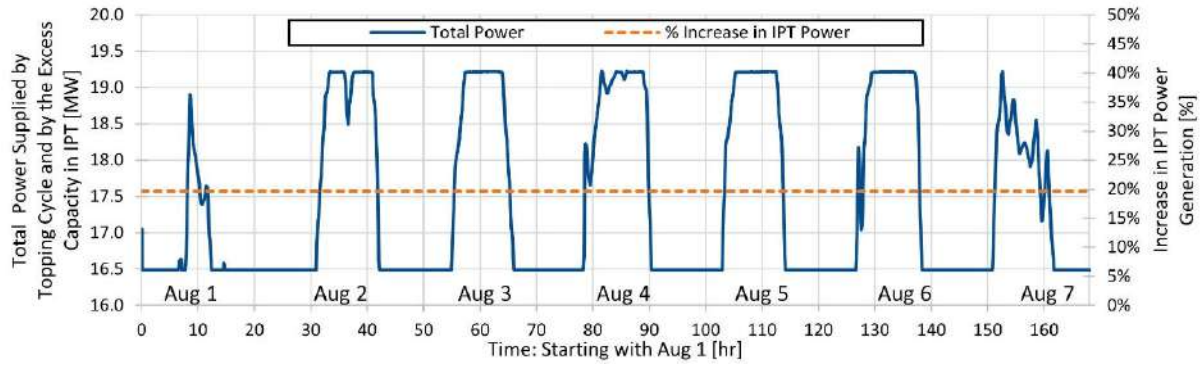
Figure 2. Total power produced by the topping CSP-biomass cycle and the increase in IPT power generation during a week in August for KZD2 GPP in Denizli, Turkiye

## References

[1] B. Mutlu, D. Baker, and F. Kazanç, "Development and Analysis of the Novel Hybridization of a Single-Flash Geothermal Power Plant with Biomass Driven sCO2-Steam Rankine Combined Cycle," *Entropy*, vol. 23, p. 766, Jun. 2021, doi: 10.3390/e23060766.

[2] U. Serpen and R. DiPippo, "Turkey - A geothermal success story: A retrospective and prospective assessment," *Geothermics*, vol. 101, p. 102370, May 2022, doi: 10.1016/j.geothermics.2022.102370.

[3] "Solar Resource Maps of Turkey," Solargis, https://solargis.com/maps-and-gis-data/download/turkey (accessed May 11, 2023).

[4] A. M. Patnode, "Simulation and performance evaluation of Parabolic Trough Solar Power plants," thesis, 2006

# Comparison of Conventional and Microwave Heating of Solar Salt

Cristóbal Valverde, Margarita M. Rodríguez-García, Esther Rojas, Rocío Bayón.

*CIEMAT - Plataforma solar de Almería*
cvalverde@psa.es

Electricity generation and thermal sector are major contributors to greenhouse gas (GHG) emissions [1]. To address decarbonisation, it is possible to decouple electricity production and consumption through commercially available thermal energy storage (TES) systems, which are already used in concentrated solar thermal power (CSTP) [2]. This can also be used to increase the contribution to the electricity network of other renewable energy sources such as solar PV and wind power plants. Carnot batteries or Power-to-Heat-to-Power systems are existing technology-based systems [3], and therefore, have a large installation potential. This is the case for connecting photovoltaic or wind power plants with CSTP plants to produce electricity in combination with industrial heat [4].

To date, TES is a technology installed in 45.5% CSTP plants with a total storage capacity of 22 $GWh_{el}$ [5]. The most widely used storage medium is solar salt, a non-eutectic mixture of 60 $_{wt}$% $NaNO_3$ and 40 $_{wt}$% $KNO_3$. When connected to wind or PV generation systems, TES designs so far assume that solar salt is heated using electric resistance heater.

For the benefit of sustainability and to improve the charging process, microwave heating is presented as a compact and cost-effective direct conversion of energy into heat with significant advantages over conventional heating. Microwaves are electromagnetic waves in the frequency band between 300 MHz and 3000 GHz, which are non-ionizing and interact directly with matter at the molecular level. This avoids the limitations derived from conduction and convection in materials with low thermal conductivity, including the possibility of an electronic control with a high response of heating medium, or instantaneous system start-ups and shut-downs [6].

So far, concerning the heating of solar salt with microwaves, Rodríguez-García et al. [7] made a first dielectric characterization by heating the solar salt at 2.45 GHz, demonstrating that it is possible to heat this liquid medium to the working temperature from 290 °C to 565 °C.

The objective of this paper is to heat liquid solar salt in two different devices: a muffle furnace and an industrial microwave oven in order to compare both heating processes in terms of

uniformity, efficiency and speed. The same conditions will be applied to both devices and the temperature reached, time and energy consumption will be recorded and compared. These experiments will be performed with different crucible materials to determine their suitability for both methods.

The devices used for the experiments are shown in Fig. 1. The muffle furnace (left) has 6 kW maximum power and can reach 1100 ºC maximum temperature and the microwave industrial oven (right) works at 3.15 kW and allows reaching 1200 ºC maximum temperature.
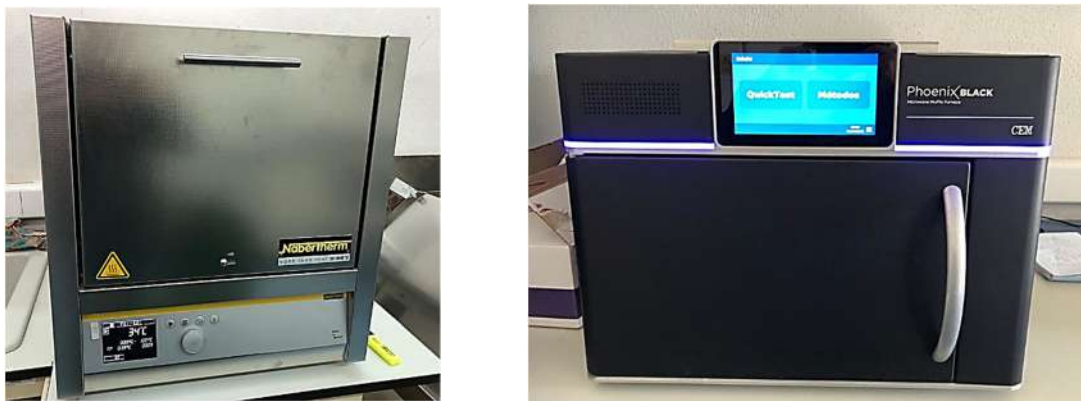


Fig. 1. Muffle furnace (left). Microwave oven (right)

Finally, by means of numerical modelling based on the finite element method (FEM), the 3D models of these cases will be built and validated from the results obtained.

[1] Low-carbon heating and cooling: overcoming one of world's most important net zero challenges; The Royal Society: United Kingdom, 2021-06-25 2021.

[2] Crespo, L. The double role of CSP plants on the future Electrical Systems. Available online: https://about.bnef.com/blog/battery-pack-prices-cited-below-100-kwh-for-the-first-time-in-2020-while-market-average-sits-at-137-kwh/ (accessed on Aug. 8).

[3] Dumont, O.; Frate, G.F.; Pillai, A.; Lecompte, S.; De Paepe, M.; Lemort, V. Carnot battery technology: A state-of-the-art review. Journal of Energy Storage 2020, 32, doi:10.1016/j.est.2020.101756.

[4] IRENA. Storage and Renewables: Costs and Markets to 2030. Abu Dhabi.: Int Renew Energy Agency 2017.

[5] DOE Global Energy Storage Database. Statistics. Available online: https://sandia.gov/ess-ssl/gesdb/public/statistics.html (accessed on 8 November).

[6] Mishra, R.R.; Sharma, A.K. Microwave-material interaction phenomena: Heating mechanisms, challenges and opportunities in material processing. Composites Part a-Applied Science and Manufacturing 2016, 81, 78-97, doi:10.1016/j.compositesa.2015.10.035.

[7] Rodriguez-García, M.M.; Bayón, R.; Alonso, E.; Rojas, E. Experimental and Theoretical Investigation on Using Microwaves for Storing Electricity in a Thermal Energy Storage Medium. In Proceedings of the SOLARPACES 2021: International Conference on Concentrating Solar Power and Chemical Energy Systems, 2021.

# Competitiveness of Carnot Batteries in power generation and industrial applications

Tiago R. Eusébio, Pedro Horta.

*Renewables Energy Chair – University of Évora*
tre@uevora.pt

Fully decarbonized power systems require the ability to balance the mismatch between energy supply and demand. The growth of non-dispatchable renewables like solar or wind power renders energy storage systems crucial to achieve electric grid flexibility, providing the needed dispatchability for the system. Given their potential competitive cost, efficiency and sustainability, Carnot batteries are a promising electricity storage solution upon charging through power to heat components at potentially low electricity costs – which might include heat upgrade through the use of heat pumps, and discharging it in the form of electricity on demand, through a suitable thermodynamic cycle turning heat into power [1].

A variety of configurations is possible, since the basic premise of a Carnot battery involves: the charge stage, where electricity can heat up the storage medium by means of a heat pump and/or an electric heating device; the storage system, which presents a variety of possible media at different temperatures; and the discharge stage, by means of a thermodynamic cycle, converting heat to electricity [1].

Depending on the operating temperatures involved, different combinations are possible, which might favor a given configuration over the other in terms of cost competitiveness, considering not only different Carnot battery configurations but also Electrochemical Electricity Storage technologies. Such assessment is furthermore to be done over a variety of configurations being researched and commercialized, as well as in a context of rapidly evolving technology costs.

Aiming at the development of a tool enabling a straightforward assessment of the most suitable Carnot Battery configurations to different operating and market conditions, this work aims at:

- developing a model enabling a yield assessment of different Carnot Battery configurations and system compositions (power to heat, thermal storage and heat to power components) working under different operation conditions (heat source, thermal storage media, load profile, charging/discharging response);

- embed an economic assessment in the model, enabling the assessment of LCOS (Levelized Cost of Storage) in view of different macroeconomic, lifetime, CAPEX and OPEX parameters;

- benchmark the technical-economic results with other electricity storage technologies (reverse pumping, Li-ion or post-Lithium EES technologies),

thus enabling the definition of customized optimal Carnot Battery configurations and the assessment of their competitiveness.

The work is organized in three major stages:

- on a first stage, information is being gathered and organized to assess the competitiveness threshold of Carnot Batteries for various conditions compared to different electrochemical storage solutions;

- a second stage involves the modelling (at component and system level) and experimental validation of a specific Carnot Battery being designed in the scope of an ongoing project (PRR ATE);

- A third stage aims at using TRNSYS for Transient or quasi-dynamic simulations, with the ability to add new models for components (based on literature and validated experimentally) coupled with Python to set routines for a parametric technical-economic assessment of different combinations of Carnot batteries.

The modelling tool developed in this work will enable the production of a technical-economic assessment of different Carnot battery configurations for a given set of conditions, namely:

- temperature levels which have an important repercussion of the heating system (electric heater, heat pumps or even a combination of both);

- the storage system (type of media, sensible versus latent heat mechanism) and

- the most suited thermodynamic cycles.

The results produced with this tool will enable the definition of competitiveness boundary conditions for Carnot Battery technologies under different operation and market conditions.


References

[1] T.Liang, A.Vecchi, K.Knobloch, A.Sciacovelli, K.Engelbrecht, Y.Li, Y.Ding, Key components for Carnot Battery: Technology review, technical barriers and selection criteria, Renewable and Sustainable Energy Reviews 163 (2022) 112478, https://doi.org/10.1016/j.rser.2022.112478.

# Developing a Digital Twin of the Solar Field of Solar Tower Plants

Maitane Ferreres Eceiza[1], Gregor Bern[1]

*[1]Fraunhofer Institut for Solar Energy Systems ISE, Heidenhofstr. 2, 79110 Freiburg im Breisgau, Germany*
*maitane.ferreres.eceiza@ise.fraunhofer.de*

To maximize the efficiency and performance of CSP plants, it is essential to continuously monitor and optimize their operation. One promising approach is the development of digital twins for CSP plants [1]. A digital twin is a virtual replica of a physical system that can simulate its behavior under different operating conditions.

By providing accurate, physics-based representations of the plant's systems and components, digital twins integrate real-time data to simulate behavior, predict performance, and instantly diagnose malfunctions and failures.

The planned doctoral dissertation aims to address several research questions related to the development and validation of digital twins for CSP plants, which can also be discussed in the context of this colloquium:

1. *How can a digital twin accurately model the optical and thermal behavior of a heliostat field and an external receiver in real time? What are the limitations and challenges of doing so?*
2. *How can a digital twin be validated using real data from a concentrated solar power plant? How can uncertainties in the digital twin models and real data be evaluated and minimized to improve the accuracy of the predictions and control strategies?*
3. *What strategies can be developed based on the predictive capabilities of the digital twin to improve plant operation in real time and mitigate the risk of unexpected failures?*

The focus of this study will be on the first step of the dissertation, namely the development of a robust digital twin for the solar field of CSP plants, ensuring a comprehensive understanding of its optical behaviour. The ultimate goal of this model is to improve the accuracy of the flux prediction on the external receiver, to develop an accurate, spatial high-resolution representation of the surface temperature of the receiver tubes.

To achieve realistic simulations of the solar field, Ray Tracing simulations are employed based on the in-house software Raytrace3D [2]. By integrating comprehensive measurements of

spatial cleanliness data, bidirectional reflectance distribution function models representing the reflective properties of soiled mirrors, mirror slope deviation affecting the surface geometry, canting errors responsible for misalignments, and tracking accuracy of heliostats, the digital twin aims to achieve high accuracy in its predictions. Neglecting deviations in these factors could introduce substantial discrepancies between the digital twin's predictions and the actual heliostat field performance in real scenarios. By incorporating these intricate details within the Ray Tracing simulations, the digital twin emerges as a powerful tool capable of providing a physics-based understanding of the solar field's behavior, reinforcing its potential to further advance plant optimisation and decision-making processes.

**References:**

 **[1]** A. Rasheed, O. San, T. Kvamsdal, *Digital twin: Values, challenges and enablers from a modeling perspective*, IEEE Access, 8 (2020), pp. 21980-22012.

**[2]** *Raytrace3d by Fraunhofer ISE. Accurate and Efficient Ray Tracing for Concentrator Optics.* P. Schöttl, G. Bern, P. Nitz, F. Torres, L. Graf. Fraunhofer Institute for Solar Energy Systems ISE, Freiburg, 2022.

# Application of AI methods to improve Operation and maintenance of CSP power plants

Thomas Kraft, Haziq Khan, Dr. Gregor Bern

*Fraunhofer Institute for Solar Energy Systems ISE*

*Mail: Thomas.kraft@ise.fraunhofer.de.*

The global significance of artificial intelligence (AI) is on the rise. Neural networks are increasingly being applied in both personal and professional settings. Moreover, the potential of AI has been explored in the field of CSP (Concentrated Solar Power). For instance, it has been utilized to predict the outlet temperature of a single collector [1] and estimate the energy production of a parabolic trough solar thermal power plant [2].

This study focuses on investigating the predictability of individual system parameters for the entire solar field, including the reaction of the solar field's outlet temperature to meteorological parameters and mass flow. The research utilizes five years of real power plant data along with a neural network (NN) implementation to achieve higher predictive accuracy. The expected outcomes are improved fault detection, enhanced predictive maintenance, and increased power plant efficiency in the long run.

This study is based on a comprehensive dataset spanning five years of operational data from a parabolic trough power plant in Spain. The power plant has an approximate nominal capacity of 50 MW for the power block and generates over 150 GWhel annually from a solar field with more than 100 hydraulically individual loops. The data is recorded at a resolution of 5 minutes over the 5-year period.

To begin, a correlation matrix was conducted to identify the most influential input parameters on the variable of interest, which is the outlet temperature. Among the parameters considered were direct normal irradiation (DNI), mass flow, and wind speed. Subsequently, a neural network (NN) was implemented and trained using the operational data of the system.

The goal was to optimize the prediction accuracy, and this involved systematically varying relevant NN hyperparameters such as the number of layers, neurons in each layer, learning rate, and batch size. Additionally, a sensitivity analysis was performed to quantify the individual effects of these parameters on the network's prediction accuracy.

Due to the time-dependent nature of the power plant processes (e.g., heating up and cooling down), recurrent neural network (RNN) and long-short-term-memory (LSTM) models were employed for parameter prediction.

Selecting the right hyperparameters is vital for optimizing the performance of a neural network. To determine the most suitable learning rate for the base scenario neural network, a balance between low error and fast convergence was sought. As a result, a learning rate of $10^{-3}$ was chosen, as it demonstrated a combination of minimal error and rapid convergence, making it the optimal choice for the neural network's performance.

By carefully selecting the training data and tuning the hyperparameters of the Neural Network, the solar field's outlet temperature could be predicted with a remarkable Mean Absolute Error (MAE) of less than 10 K. The prediction accuracy, however, is not consistent throughout the day but exhibits significant fluctuations. While the network can accurately predict constant temperatures during the day, deviations increase notably during the start-up and shut-down processes, as well as during the night.

These observations highlight that the neural network's performance is affected by the dynamic nature of the solar field's behavior. Predicting temperatures during periods of stable operation is relatively accurate, but challenges arise during transitional phases and night-time conditions. Further research and adjustments might be necessary to enhance the network's prediction capabilities during these specific scenarios

## References

[1] M. Cervantes-Bobadilla et al., "Control scheme formulation for a parabolic trough collector using inverse artificial neural networks and particle swarm optimization," J Braz. Soc. Mech. Sci. Eng., vol. 43, no. 4, 2021, doi: 10.1007/s40430-021-02862-4.

[2] A. Zaaoumi et al., "Estimation of the energy production of a parabolic trough solar thermal power plant using analytical and artificial neural networks models," Renewable Energy, vol. 170, pp. 620–638, 2021, doi: 10.1016/j.renene.2021.01.129.

# Condition Monitoring for Heliostat Fields using Artificial Intelligence

Dominik Steinberg[1], Marc Röger[2], Daniel Maldonado Quinto[3]

[1]*German Aerospace Center (DLR), Institute of Solar Research,*
*Karl-Heinz-Beckurts-Str. 13, 52428 Juelich, Germany*

[2]*German Aerospace Center (DLR), Institute of Solar Research,*
*Paseo de Almería 73, 04001 Almería, Spain*

[3]*German Aerospace Center (DLR), Institute of Solar Research,*
*Linder Höhe, 51147 Cologne, Germany*

dominik.steinberg@dlr.de

For the efficient operation of solar power tower plants, it is of great importance to ensure high reliability of the large number of individual heliostats within the heliostat field. By using real-time sensor data from the heliostat field, a condition monitoring system can be developed that enables automated fault detection and early detection of ageing effects such as wear. For this data-driven analysis, however, it is difficult to collect comprehensive and sufficient measurement data for the entire heliostat field, as not every single heliostat can be equipped with high-resolution, expensive sensors. In addition, the information implicit in the measurement data must be extracted from various data sources and combined in a suitable manner to accurately characterise the operating conditions of the heliostats. Therefore, it is important to identify which relevant status data can be obtained with low-cost measurement sensors and how this process can be complemented utilizing so-called virtual sensors that generate detailed insights of the heliostat operating status by cleverly combining easily accessible information. Motivated by the outstanding success of Artificial Intelligence (AI) in other research areas, the aim is also to investigate which specific AI techniques can best be used to develop the condition monitoring system that replaces labour-intensive manual damage detection with predictive maintenance. This contribution aims to provide a detailed overview of the current state of research in condition monitoring techniques for heliostats. In addition, an outlook on a new methodology focusing on machine learning-based evaluation of time series sensor data from heliostat drives, motors and controller units is presented. The goal of this method is to derive valuable insights from the sensor data and to identify opportunities for virtual sensors using existing/low-cost sensors.

# IoT and Big Data platforms as the basis for autonomous complex systems in Industry 4.0

Inga Miadowicz

*Deutsche Luft- und Raumfahrt (DLR)*
*Inga.Miadowicz@dlr.de*

With increasing digitization in the age of Industry 4.0, highly automated, semi-autonomous and, in the future, fully autonomous systems are emerging [1]. These contribute to improving industrial productivity, reducing costs and allowing an environment-, energy- and resource-saving production at the same time [2].

To allow systems to work autonomously in the future, a suitable infrastructure is required that enables autonomous control algorithms to solve tasks flexibly, in acceptable time, under changing environmental influences and with little or no input from humans [1]. As a basis for this they rely on high quality data, interconnections to other subsystems, human interfaces, as well as a secure and reliable overall system environment. The infrastructure lays the technological foundation for the ability of autonomous algorithms to act and control independently according to the requirements. It is an important basis for the effective further development of the degree of autonomy in industrial systems [3].

Especially for extensive industrial systems, which are composed of heterogeneous, volatile sub- and legacy systems, the implementation of data and infrastructure requirements is challenging with an increasing degree of automation [4]. A lot of data sources, large amount of operating data, networking of heterogeneous system components, continuous further development of the infrastructure, as well as high requirements for latency, safety and reliability make the development of autonomous systems extremely demanding, if no suitable overall architecture concept is being used.
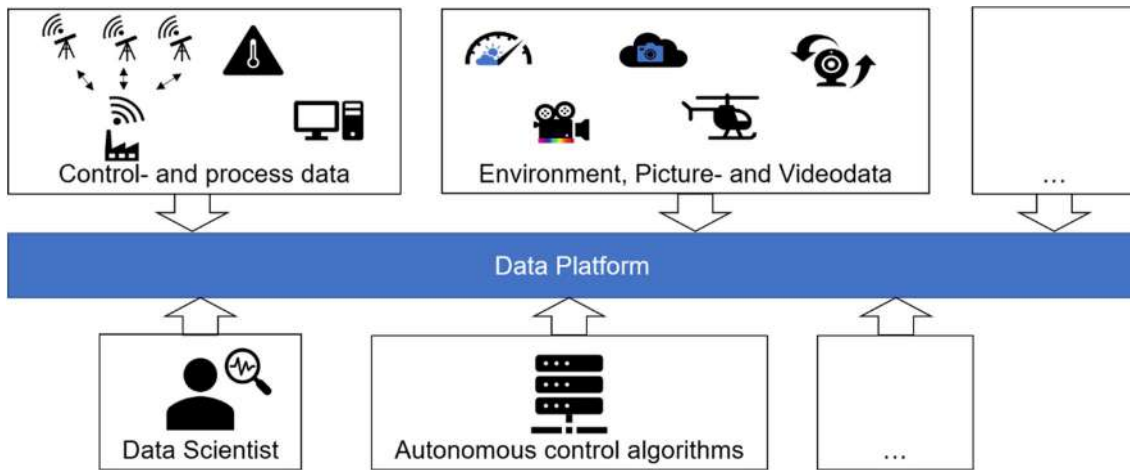
*Figure 1: High-Level-View Data Platform*

Therefore, a system architecture for a data platform as the basis for autonomous complex systems in industrial environments is being developed as part of the PhD project. The goal is to determine the potential and requirements of data platforms for autonomous systems, to develop a generally applicable solution concept, and to implement and evaluate this in the context of a (partially) autonomous solar thermal power plant. The result proposes a solution and shows to what extent the proposed platform architecture can improve the system operation and contribute to increasing the degree of autonomy of complex industrial systems.

**Literature sources**

[1]      Radhya Sahal., John G. Breslin, Muhammad Intizar Ali: *Big data and stream processing platforms for Industry 4.0 requirements mapping for a predictive maintenance use case*, Journal of Manufacturing Systems, 54 (2020) 138-151.

[2]      Hualong Chen, Wen Yuanqiao, Zhu Man, Huang Yamin, Xiao Changshi, Wei Tao, Axel Hahn: *From Automation System to Autonomous System: An Architecture Perspective*, Journal of Marine Science an Engineering, 9 (2021), 645.

[4]      Hartmut Hirsch-Kreinsen, Anemari Karacic*: Autonome Systeme and Arbeit: Perspektiven, Herausforderungen and Grenzen der Künstlichen Intelligenz in der Arbeitswelt*, Bielefeld, transcript, 2019.

[5]      Keliang Zhou, Taigang Liu, Lifeng Zhou: *Industry 4.0: Towards Future Industrial Opportunities and Challenges*, 2015 12th International Conference on Fuzzy Systems and Knowledge Discovery (FSKD), Zhangjiajie, China, 2015, 2147-2152.

# Simulation Environment for Developing and Testing UAV-Based CSP Condition Monitoring Systems

Alexander Schnerring[1,2], Rafal Broda[1,2], Julian J. Krauth[1], Marc Röger[1], Robert Pitz-Paal[1,2]

[1]*German Aerospace Center (DLR), Institute of Solar Research*
[2]*RWTH Aachen University, Chair of Solar Technology*
*alexander.schnerring@dlr.de*

In central receiver concentrating solar power (CSP) plants, several thousand mirrors (so-called heliostats) focus solar radiation onto a receiver mounted on a central tower. The efficiency of such plants is negatively affected by falsely aligned and damaged heliostats. Hence, the condition of the power plant has to be monitored in order to ensure cost efficient operation. A common approach is to use unmanned aerial vehicles (UAVs) to perform this task. Currently, flight routes for these UAVs are planned prior to their flight, while measurement data is evaluated after the flight. This comes with the disadvantage that insufficient measurement data quality often is only recognized when the UAV has already landed. For this reason, we are working on performing the image data analysis in real-time (i.e. while the UAV is still flying), enabling the dynamic planning of the UAV flight route based on data analysis results and opening up new possibilities for automated monitoring. The development cycle of UAV-based measurement systems consists of several recurring steps: The implementation of new features is followed by test measurements, analysis and problem identification. Based on this, potential bugs are fixed and features are further developed. However, field tests are time-intensive, not always successful and always pose a risk of material damage.

We propose to mitigate these problems using a simulation environment in which CSP condition monitoring systems can be developed and tested prior to their application in the real world. Our implementation is based on the physics game engine *Unreal Engine*. Through additional software, the simulated drone can be controlled with the same commands as a real drone, facilitating the prototyping of flight route planning. In addition, the simulation allows for the precise modeling of heliostat geometries and positions as well as the control of heliostat

orientations. This system lays the foundation for the development of real-time image-based

Fig.1. The simulated drone is controlled inside a virtual environment. The simulation allows for the modeling of a heliostat field and real-time sampling of both, camera position and image data.

condition monitoring tasks: Image data can be easily sampled from the simulation while the ground truth camera position and orientation are available, providing a framework for the evaluation of image-based algorithms such as the localization of the camera and heliostat outlier detection.

# Using Synthetic Data for Developing Deep Learning Based Airborne Monitoring Methods for Solar Tower Power Plants

Rafal Broda[1,2], Alexander Schnerring[1,2], Julian J. Krauth[1], Marc Röger[1], Robert Pitz-Paal[1,2]

*[1]German Aerospace Center (DLR), Institute of Solar Research*
*[2]RWTH Aachen University, Chair of Solar Technology*
*rafal.broda@dlr.de*

Solar tower power plants utilize between 1000 and more than 100,000 mirrors, so-called heliostats, to concentrate solar irradiance onto a central tower receiver. For a reliable and efficient operation, regular monitoring of these heliostats is essential. Key operational parameters include their precise alignment to ensure that the irradiance is accurately directed towards the receiver, as well as the condition of the mirror surfaces. For fast and cost-effective monitoring, drones equipped with high-resolution cameras are increasingly being developed and used. They capture images of the heliostat field, which are then analyzed by image processing methods. While conventional image processing techniques show promising results, they do not offer the required speed and flexibility for handling challenges such as varying lighting conditions, damaged or soiled mirrors and reflections. They often also require manual intervention, adding complexity and cost to the process.

To address these challenges, we aim to leverage deep learning methods, which have proven themselves against conventional algorithms in many domains over the past decade. Our focus lies on developing models to solve various detection tasks related to heliostat monitoring. A special aspect of our approach is the generation of synthetic image data for training our models. We use a simulation environment based on *Blender* and *BlenderProc* to create artificial scenes of heliostat fields and to render photorealistic images along with ground truth labels. This way we get access to large amounts of training data essential for developing effective deep learning models. Furthermore, it allows us to simulate operationally relevant scenarios in a wide variety of situations difficult to replicate in real plants. We train a state-of-the-art deep-learning model for mirror surface and mirror facet corner point detection using only synthetic data and apply it to a real-world image of a heliostat field. In this presentation we show our promising preliminary results [1], demonstrating the applicability of our approach.

Fig.1. Example image from our simulation environment. The random compilation of our scenes helps to overcome the reality gap when training deep learning models.

[1] R. Broda, A. Schnerring, J.J. Krauth, M. Röger, R. Pitz-Paal, *Proc. of SPIE*, 2023, submitted

# Characterization and Optimization of High Reflectivity Mirrors for Solar Towers

Eslem Enis Atak

*Middle East Technical University*
eatak@metu.edu.tr

Concentrated Solar Power (CSP) is a fast-developing area in solar energy. A solar tower based CSP plant has four main components: receiver, tower, power block, and heliostat field. A heliostat is tracking device with a reflector on top, which turns to keep the sunlight concentrated at the receiver. The performance of reflectors is important crucial for CSP performance since they directly determine the amount of light that can be concentrated, i.e., converted to heat. Solar reflectors degrade over time and need periodic replacement. Since CSP plants cover large areas, the cost of replacing reflectors cannot be underestimated. Reflectors in heliostat fields are exposed to a variety of environmental deformation mechanisms: ultraviolet (UV) radiation, temperature cycling, abrasives like dust and sand, humidity, and mechanical stresses. Their long-term optical performance (i.e., aging behavior) should be determined before large scale operations. However, fundamental understanding of mirror aging is lacking. Degradation of optical properties are not linked to micro mechanical characteristics (such as micro-defects) and their propagation. A reliable model that correlates weather and climate conditions to aging is needed. Therefore, this thesis will focus on developing a reliable aging model to correlate mechanical properties to optical properties. The expected outcomes of this study are:

- Determine the mechanical degradation through studying the dynamics of the defect propagation process induced due to mirror operation and exposure to the environment.
- Determine the relationship between mechanical degradation, wetting, and specular reflectivity Develop a numerical model to estimate performance in different sites with different weather conditions.
- Optimize the mirrors for maximum reflectivity, minimum cost, and maximum durability
- Develop mirrors for effective use for both beams down central receiver and heliostat applications.
- Reduce the copper content in mirrors for more environmentally friendly designs.

The study will consist of several stages. At first stage, mirror samples will be obtained and existing defects will be studied though microscopy and the optical properties will be characterized by reflectometry and spectroscopy. The reflectors will be exposed to both natural and artificial aging processes. Using the collected data over years, numerical models will be established and reflector designs will be optimized for reflectivity, duration and cost.

# Spectral analysis and ray tracing of Fresnel solar furnace model (PSA) using OTSun software

N. Estremera-Pedriza, J. Fernández-Reche

*CIEMAT-Plataforma Solar de Almería. noelia.estremera@psa.es*

The Plataforma Solar de Almería (PSA) is studying how to improve the efficiency of solar thermal tower power plants due to the importance they have today, as they not only generate electricity during the day, but can also store heat for use and generate electricity during hours when there is no sun, such as at night. One of the studies being carried out is to analyse whether there is a dependence between wavelengths and the ageing of the material used in the receiver of some tower power plants. For this study, experimental tests are being carried out in alloy 625 plates in the PSA's new Fresnel furnace [1]. This facility uses two types of selective reflectance mirrors, the first mirror filters most of the wavelengths between 400 nm and 1125 nm (101 × 127mm) [2], whereas the second one filters part of the wavelengths between 700 nm and 10000 nm, it is 50 mm of diameter and has a protective layer of gold that is responsible for the selective filtering [2]. The purpose of these mirrors is either remove part of the visible and mid-IR wavelengths, in the first case, and remove the UV and a small part of the visible wavelengths in the second one [3]. Therefore, in order to provide more information to the study, simulations of the Fresnel solar furnace are being carried out with the OTSun software [4] with the aim of knowing the power that will reach the material with each mirror.

Thus, all the components of the Fresnel solar furnace have been modelled and all the optical properties of its component materials have been introduced in the software. The advantage of the simulation software consits on the posibilitie to carry out wavelength dependend simulations, not provided for any other ray tracing simulation softwares.



(a)                                           (b)
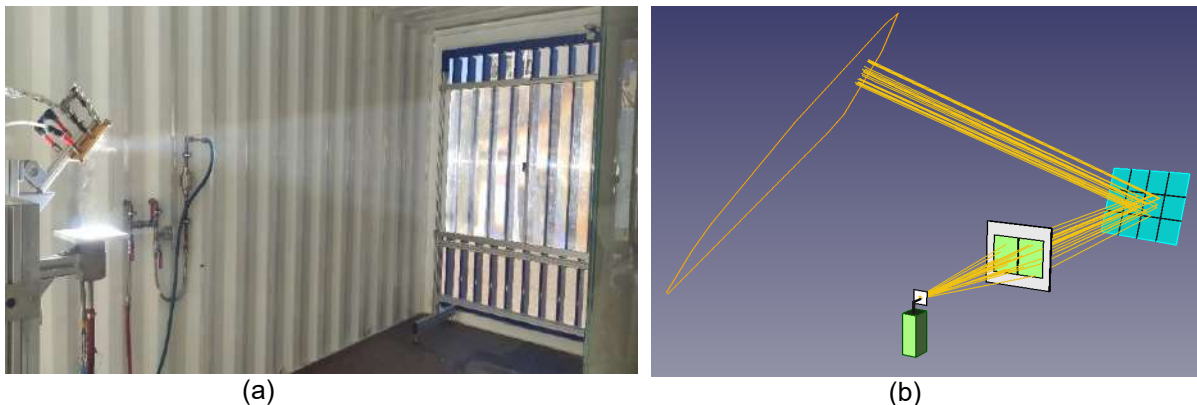
*Fig. 1: (a) Picture of the Fresnel solar furnace in operation, and (b) Ray tracing of the Fresnel solar furnace facility under OTSun*

To validate the model, first, data from the simulation of the base model are compared with the data obtained in the characterisation performed on a specific day of the Fresnel lens [1].

And, as final result, ray tracing and spectral analysis results are obtained that reveal the power reaching the material with each mirror. Table 1 compares power simulation results with both mirrors.

*Table 1. Comparative table of characterisation results and simulated results in OTSun.*

| | | Base-Lamb | Mirror 3 | Mirror 6 |
|---|---|---|---|---|
| **Characterisation Results** | Standard Spectrum (%) | 100 | 66.46 | 35.76 |
| | DNI std ($W/m^2$) | 892.30 | 593.05 | 319.07 |
| | DNI caract ($W/m^2$) | 873.40 | 580.49 | 312.31 |
| | Radio 90% Energy Charact (cm) | 2.7cm (100% - 3.8 cm) | - | - |
| | Total Power (kW) | 1.13 | - | - |
| | Peak Power ($kW/m^2$) | 1134.9 | - | - |
| **OTSun Simulation Results** | Radio 90% Energy OTSun (cm) | 4.01 cm | 4.31 | 5.20 cm |
| | Total Power OTSun (KW) | 1.135 | 0.60 | 0.50 |
| | % Reduced Power | - | 56.01 | 46.81 |
| | Peak Power ($kW/m^2$) | 904 | 247 | 242 |
| | % Reduced Peak Power | - | 73.23 | 72.68 |

The base model has been validated agains the experimental data obtained in the characterization campaign comparing the data of Table 1, colum Base-Lamb, between Characterization results and OTSun simulation results, taking into account that the exact geometry of the Fresnel lens is not known. As a summary of the models for the two mirrors, the values of radius, power and peak power have been shown. After aging of alloy 625 plates with both mirrors, further studies with Ansys Fluent will be necessary to correlate these values of both mirrors with the temperature and ageing of the material.

**Acknowledgment**

**References**

[1] Estremera-Pedriza N, Fernández-Reche J, Carballo JA. "Optical Characterization of a New Facility for Materials Testing under Concentrated Wavelength-Filtered Solar Radiation Fluxes". Solar. 2023;3(1):76–86.
[2] Edmund Optics Europe, URL: https://www.edmundoptics.eu/?gclid=EAIaIQobChMIPmE6t7o9gIVCJ7VCh31Cg66EAAYASAAEgJ5qfD_BwE. Last access July 15, 2023.
[3] E. Setien, J. Fernández-Reche, M. Álvarez-de-Lara, and M. J. Ariza, "Experimental system for long term aging of highly irradiated tube type receivers," Sol. Energy, vol. 105, pp. 303–313, 2014, July, 2014, doi: 10.1016/j.solener.2014.04.004.
[4] Pujol-Nadal R, Cardona G. "OTSunWebApp: A ray tracing web application for the analysis of concentrating solar-thermal and photovoltaic solar cells". SoftwareX [Internet]. 2023;23:101449. Available from: https://doi.org/10.1016/j.softx.2023.101449

# Development of Switchable Technology for Agrivoltaic

Rebecca Cizek, Kai Gehrke, Florian Sutter, Eckhard Lüpfert, Robert Pitz-Paal

*DLR German Aerospace Center*
*Institute of Solar Research*
*rebecca.cizek@dlr.de*

Photovoltaic modules as roof for large greenhouses can produce clean electricity and regulate the temperature and irradiance for the crops to increase production. Reversible metal electrodeposition [1] is used to create switchable windows powered by planar integrated transparent solar cells [2,3] for greenhouse application. The proposed technology aims to create an autonomous system capable of self-regulating its transparency based on solar irradiation, helping to control the temperature inside the greenhouse, especially during high irradiation periods.

The whole system is divided into two parts. One is the switchable window which consists of an electrolyte enclosed by two transparent electrodes and a protective cover, such as glass or foil. The other one is a transparent thin film solar cell designed with a p-i-n stack.
The functionality of the switchable window relies on the inclusion of metal ions ($M^{n+}$) into the electrolyte. Those ions ($M^{n+}$) reduce to metal ($M$) by using the electrons ($e^-$) provided by the negative charged electrode.

$$M^{n+} + ne^- \rightleftharpoons M \qquad n \in \mathbb{N}$$
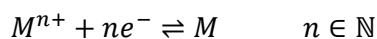
Using copper as a metal enhances the bleaching process [4,5,6] but the deposited layer would seem reddish [7]. For the application in greenhouses a layer with a medium transparency could help regulate the heat inside while still allowing sunlight for the plants. To achieve this tin is added as a metal into the electrolyte. Together with copper it will form a greyish layer on the electrode when the voltage is about -0.9V [7]. When the applied voltage reaches -1.5V the copper and tin form bronze, which causes a mirror-like deposit [7]. Additionally, lithium is added to the electrolyte to increase the ionic conductivity [8]. It also works as
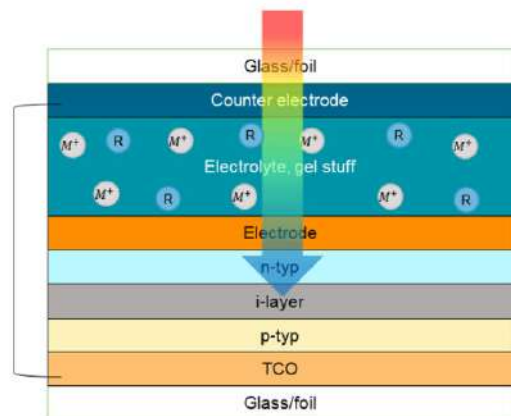


Figure 1: Bleached state of switchable window with integrated solar cell. $R$ represents the counter part to the metal ions ($M^+$). The sunlight is transmitted through the electrolyte to the transparent solar cell.
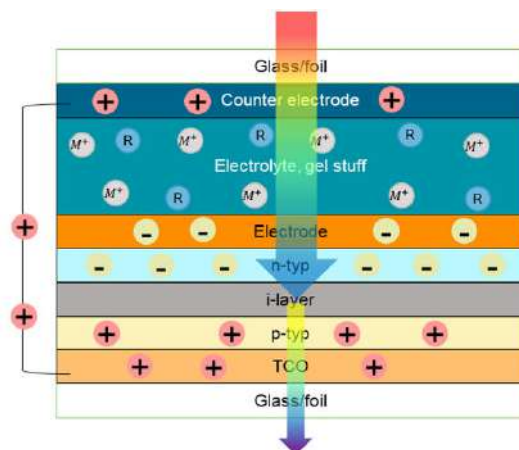


Figure 2: The transparent solar cell converts the infrared spectrum of the sunlight to electrons (-) and holes (+). The charge spreads into the related layers to the electrode and counter electrode of the switchable window.

the counter part for the metal ions. The lithium oxidizes to $Li^+$ on the other electrode by losing electrons ($e^-$)

$$Li \leftrightarrows Li^{n+} + ne^- \qquad n \in \mathbb{N}$$

and completing the redox reaction [9]. The reversed process could be achieved by applying a positive voltage of at least the same amount to bleach the electrodes. Alternatively, without applied voltage the electrode will bleach by itself over time.

Further ingredients of the electrolyte are dimethyl sulfoxide (DMSO) and polyvinyl alcohol (PVA) [10]. The PVA helps to stabilize the electrolyte in a freezing-thawing process to create a solid-like gel [10].

The solar cell consists of silicon and germanium multilayers deposited through plasma enhanced chemical vapor deposition (PECVD). The ultrathin layers are about 5-7 nm thick. [3]. The best stack of the solar cell for the here mentioned application is still under intense research.

Placing the solar cell behind the switchable window will achieve self-sustainability through a dynamic equilibrium between the solar-powered darkening process and the self-bleaching capability of the electrolyte.
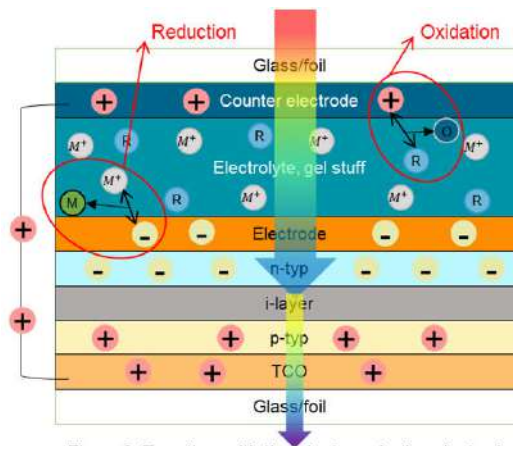


Figure 3: Together with the electrons in the electrode and metal ions in the electrolyte a reduction process takes place, creating a metal deposit. The counter reaction (oxidation) takes place on the other electrode, creating an oxide.
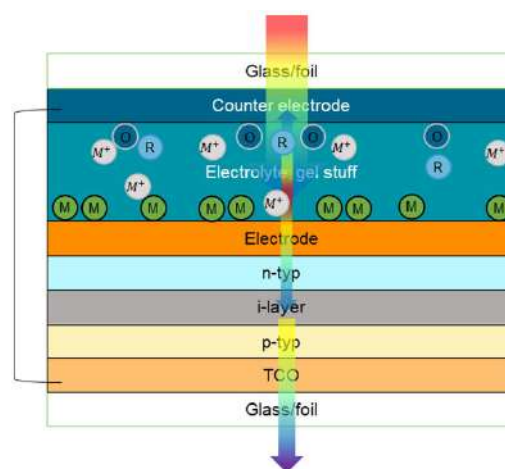


Figure 4: The metal layer can only be remained by a constant applied voltage of a certain amount depending on the composition of the electrolyte. Otherwise the metal will dissolve creating metal ions and electrons. The oxide will use the free electrons from the metals to reform the counter part of the metal ions. As soon as some of the metal layer is removed sunlight can enter the solar cell.

[1] T. S. Hernandez et al., Joule, vol. 4. Elsevier BV, pp. 1501–1513, Jul. 2020.

[2] A. L. Dyer, R. H. Bulloch, Y. Zhou, B. Kippelen, J. R. Reynolds, and F. Zhang, Advanced Materials, vol. 26, no. 28, pp. 4895–4900, May 2014.

[3] M. Gotz-Kohler, H. Meddeb, K. Gehrke, M. Vehse, and C. Agert, IEEE Journal of Photovoltaics, vol. 11, no. 6, pp. 1388–1394, Nov. 2021.

[4] X. Zhao, A. Aili, D. Zhao, D. Xu, X. Yin, and R. Yang, Cell Reports Physical Science, vol. 3. Elsevier BV, p. 100853, Apr. 2022.

[5] T. S. Hernandez, C. J. Barile, M. T. Strand, T. E. Dayrit, D. J. Slotcavage, and M. D. McGehee, ACS Energy Letters, vol. 3. American Chemical Society (ACS), pp. 104–111, Dec. 2017.

[6] X. Tao, D. Liu, T. Liu, Z. Meng, J. Yu, and H. Cheng, Advanced Functional Materials, vol. 32. Wiley, p. 2202661, Jun. 2022.

[7] A. L.-S. Eh et al., Advanced Science, vol. 7. Wiley, p. 1903198, May 2020.

[8] C. J. Barile, D. J. Slotcavage, J. Hou, M. T. Strand, T. S. Hernandez, and M. D. McGehee, Joule, vol. 1. Elsevier BV, pp. 133–145, Sep. 2017.

[9] X. Tao, D. Liu, J. Yu, and H. Cheng, Advanced Optical Materials, vol. 9. Wiley, p. 2001847, Feb. 2021.

[10] X. Guo et al., Advanced Materials Interfaces, Apr. 2023.

# Towards the optimal coupling of multi-effect distillation with solar energy

Juan Miguel Serrano, Lidia Roca, Patricia Palenzuela

*CIEMAT-Plataforma Solar de Almería-CIESOL, Ctra. de Senés km 4.5, 04200 Tabernas, Spain*
jmserrano@psa.es

In the quest for sustainable brine concentration and desalination technologies, reducing dependence on fossil fuels has emerged as a key goal [1]. One promising approach is the integration of Multi-Effect Distillation (MED) driven by alternative energy sources such as waste heat from industrial processes and/or solar thermal energy, either for stand-alone brine valorization and water production or as part of a combined electricity and water co-generation system [2].

Conventional MED plant operation focuses on maximizing the volume of distillate per unit of energy consumed at its nominal design conditions, where the plant is assumed to operate optimally. However, this approach overlooks the energy variability associated with renewable and waste heat sources, and does not take into account the availability and capacity of thermal storage, leading to significant energy waste and requiring oversizing of the solar field [3]. To address these challenges and to allow an optimal coupling of MED plants with solar energy, a hierarchical control scheme [4] is proposed, which will be developed and experimentally validated at Plataforma Solar de Almería, in a pilot MED plant coupled with a flat plate collector field and thermal storage, as shown in Figure 1 - top.

It is a two-layer architecture (see Figure 1 - bottom); the *optimization layer* takes into account all the inputs that can affect the system: environmental conditions, previous system state, cost context, etc., and by evaluating a simulation of the combined system (*simulated system*), it produces optimal references to be followed by the low-level *control layer*. This approach requires the modeling of all subsystems, the definition of an objective function, the implementation of control strategies for the control layer and the resolution of the optimization problem; and finally, the conditioning of the experimental system to apply and validate the strategy. This work presents the first implementation of the proposed scheme, in simulation. It includes the validated subsystem models, the integration of these into a complete system model and the implementation of an initial optimization layer.
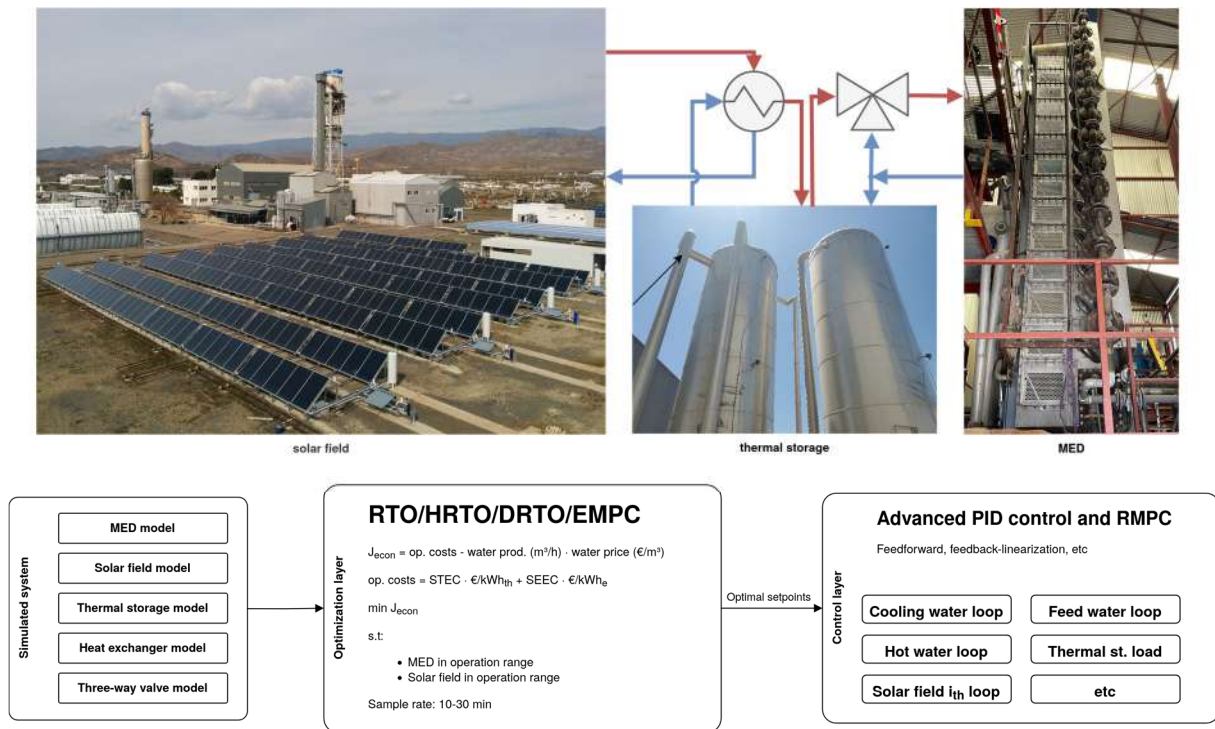
Figure 2: Conceptual diagram of proposed strategy with experimental facilities (top) and architecture (bottom)

[1] E. Jones, M. Qadir, M. T. H. van Vliet, V. Smakhtin, and S. Kang, Science of The Total Environment, 657 (2019) 1343–1356

[2] Concentrating Solar Power and Desalination Plants, P. Palenzuela, D.-C. Alarcón-Padilla, and G. Zaragoza, Springer, 2015.

[3] Mistry H., John Lienhard. An Economics-Based Second Law Efficiency. Entropy 15, no. 7 (2013) 2736–65.

[4] Albus, J.S., Barbera, A.J. and Nagel, R.N., in Theory and practice of hierarchical control, United State of America, National Bureau of Standards, 1980, 18-39.

# ASSESSMENT OF TWO SOLAR PHOTOREACTOR´S DESIGN FOR WATER DECONTAMINATION USING PHOTO FENTON REACTIONS.

K.J. Castañeda Retavizca[1], M.I. Polo-López[1,2], S. Malato[1,2].

*¹CIEMAT- Plataforma Solar de Almería, Ctra. De Senés s/n, 04200 Tabernas, Almería (Spain),*
*²CIESOL, Joint Centre of the University of Almería-CIEMAT, Almería, Spain.*
*kelly.castaneda@psa.es*

Photocatalytic solar collectors can be defined as a technology that efficiently captures solar photons and introduces them into a suitable photoreactor to promote specific catalytic reactions, which has applications in the decontamination of water, among others. Compound parabolic concentrators (CPCs) are static collectors with a parabolic reflecting surface around a cylindrical reactor tube (Fig 1.a) whose main advantage for photocatalysis is that the geometry of the reflector reflects direct light onto the receiver tube without solar tracking and has a large surface of absorber due to its low concentration ratio. They can therefore capture both direct and diffuse sunlight and were developed a long time ago [1].

At the Plataforma Solar de Almería (PSA), changes to the well-known CPC have been proposed to evaluate the possibility of decreasing the cost-benefit ratio of the solar technology, with a new photo reactor design called U-trough (Fig 1.b).
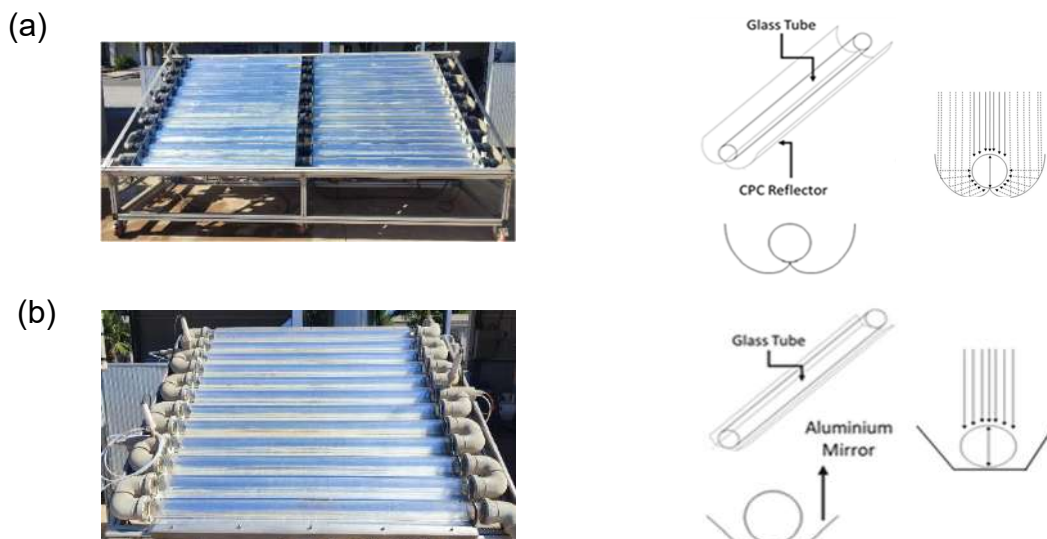


**Fig.1** (a) Photo of CPC reactor and diagram of the system. (b) Photo of V-trough reactor and diagram of system

Among the modifications proposed are: i) changing the shape of the reflecting surface to flat U-shaped reflectors, ii) increasing the diameter of the tubes from 50 mm in the CPC to 75 mm

in the U-trough, which increased the ratio illuminated volume/collector surface. Other conditions were maintained such as inclined at 37º, materials resistant to outdoor conditions, photoreactor made of commercial borosilicate Schott-Duran® glass with a UVA transmittance of 89-90% and reflectors made of anodised aluminium (Miro Sun®, Alanod, Germany), with an overall UVA reflectivity of 95%.

In this work, the two solar collectors have been compared using the solar photo Fenton reaction, where Fenton reaction and solar light are combined in the presence of hydrogen peroxide ($H_2O_2$) which provides hydroxyl radicals. The experimental conditions were the same for both reactors: 50 mg/L of contaminant (sulfamethoxazole), different concentrations of iron (7.5, 10 and 20 mg/L), 400 mg/L $H_2O_2$, natural water and 2 hours treatment time. Parameters for the comparison of the reactors were (i) iron concentration, (ii) mineralisation of contaminant and (iii) $H_2O_2$ consumption. Results were analysed using experimental time and solar UVA energy received by the solar collector per total volume of treated water.

The results showed that the optimum iron concentration in the U-trough reactor is between 7.5 y 10 mg/L Fe $^{3+}$, A lower iron concentration than in CPC with a diameter of the tubes of 50 mm. These results are consistent with well-known statements [1], as larger photoreactor diameters result in a lower optimum concentration of iron, due to lower iron concentration needs longer light path length to absorb all incident photons.

The addition of $H_2O_2$ controls the degree of mineralisation in the reaction. Therefore, in both reactors the same concentration of $H_2O_2$ was added and 80% mineralisation was achieved. However, in the U-trough reactor the energy needed to obtain similar results to the CPC was lower. This can be explained by the fact that the ratio of illuminated volume/collector surface was larger in the U-trough reactor and changing the shape of the reflecting surface did not substantially decrease efficiency.

These results indicate that the photocatalytic treatment by photo-Fenton in the U-trough reactor is more efficient than in the CPC by a proper selection of catalyst concentration, having a favourable cost-benefit ratio, as the investment costs are reduced by using a simpler reflective surface. Costs can also be decreased as a greater volume of water is being treated per collector's surface.

[1] Malato, S., Fernández-Ibáñez, P., Maldonado, M. I., Blanco, J., & Gernjak, W. (2009). Decontamination and disinfection of water by solar photocatalysis: recent overview and trends. Catalysis today.

# A competitive sustainable solution to treat WWTP secondary effluent for reusing in agriculture: chlor-photo-Fenton

Solaima Belachqer-El Attar[1,2], Paula Soriano-Molina[1,2], Agustín París-Reche[1,2], Eva Jambrina-Hernández[1], A. Agüera[1], José Antonio Sánchez Pérez[1,2]

[1]*Solar Energy Research Centre (CIESOL), Joint Centre University of Almería-CIEMAT,*
[2]*Chemical Engineering Department, University of Almería.*

*sbe146@ual.es*

Wastewater reclamation plays a crucial role in the water cycle management within a circular economy framework. Hence, the implementation of tertiary treatments in the wastewater treatment plants (WWTPs) has become an essential stage to produce reclaimed water for reusing in agricultural irrigation. Above all, when the European Union (EU) 2020/741 [1] has intensified the requirements regarding the microbiological water quality in order to guarantee the safe use and management of reclaimed water, including, in addition to *Escherichia coli* (*E. coli*), more resistant indicator microorganisms such as *Clostridium perfringens* spores and coliphages with disinfection targets ≥5 log-units. Furthermore, the regulation considers substances of emerging concern, such as microcontaminants, in the risk management plan, as there is scientific evidence of the hazard they imply for the environment and human and animal health [2]. Under these circumstances, the development of new treatments and/or technologies to comply with the regulation that, in addition to being environmentally sustainable and low-cost, do not form hazardous by-products or involve high energy costs such as conventional treatments currently implemented, chlorination and ozonation. In this regard, the solar chlor-photo-Fenton process stands out as a novel strategy based on the concurrent addition of hydrogen peroxide ($H_2O_2$) and sodium hypochlorite (NaOCl) along with ferric nitriloacetic ($Fe^{3+}$-NTA) as iron source has recently been proposed with successful results [3].

Actual secondary effluents from different WWTPs (urban and rural) located in Almería (Spain) have been treated using solar chlor-photo-Fenton with reagent concentrations of 0.1 mM $Fe^{3+}$-NTA (molar ratio 1:1), 25 mg/L $H_2O_2$ (0.73 mM of $H_2O_2$) and 10 mg/L of NaOCl (0.13 mM of NaOCl). Firstly, the treatment was applied in automatic raceway pond reactors (RPRs) at pilot scale with capacities of 0.02 and 0.08 $m^3$ (5 and 10-cm liquid depth), and subsequently, in a demonstration-scale RPR of a maximum capacity of 7.4 $m^3$ (10, 15 and 20-cm liquid depth), operated in continuous flow mode with a 1-h hydraulic residence time. During the treatment,

organic microcontaminants were quantified. As for disinfection, in addition to the indicator microorganisms (*E. coli*, coliphages and *Clostridium perfringens*) other unregulated (total coliforms and *Enterococcus faecalis*) were also quantified. On the other hand, chlorination disinfection by-products, trihalomethanes (THMs) and haloacetic acids (HAAs) were also analyzed and monitored throughout the process.

The operational feasibility of this strategy has been demonstrated by operating two consecutive days, highlighting its great potential as a tertiary treatment according to EU 2020/741. More than 75% of the total load of organic microcontaminants was removed and considering the microorganism concentration of the wastewater entering to the WWTP, the total disinfection levels achieved were ≥5 log-units for *E. coli* and coliphages, 2.8 for total coliforms, 4.7 for *Enterococcus faecalis*, 3 for *Clostridium perfringens*. On a demonstration-scale, the total disinfection levels achieved were ≥5 log-units for *E. coli* and 3 for *Clostridium perfringens*, validating that obtained at pilot scale. Concerning the microcontaminants, between 50% and 60% of the total load was removed, remarking the impact of wastewater matrix on decontamination.

Adjusting the oxidation conditions, the chlor-photo-Fenton process is shown as a promising solution for the regeneration of secondary effluents from WWTP for the most restrictive quality (Class A). Furthermore, the concentrations of *E. coli* meet the monitoring requirements for Class A, and those of THMs and HAAs, being well below the established limit [4].

**References**

[1] REGULATION (EU), 2020. 741 OF THE EUROPEAN PARLIAMENT AND OF THE COUNCIL of 25 May 2020 on minimum requirements for water reuse. Official Journal of the European Union. L 177/32, 5.6.2020.

[2] L. Rizzo, W. Gernjak, P. Krzeminski, S. Malato, C. S. McArdell, J. A. Sanchez Perez, H. Schaar, D. Fatta-Kassinos,Sci. Total, Environ. 710, (2020) 136312.

[3] S. Belachqer-El Attar, P. Soriano-Molina, I. De la Obra, J.A. Sánchez-Pérez. Sci. Total. Environ. (2022), 155273.

[4] Norme tecniche per il riutilizzo delle acque reflue, 99, 1, 3 aprile 2006, n. 152.

# Design and simulation of a model-based control system for the automated operation of the solar photo-Fenton process

D. Rodríguez-García, P. Soriano-Molina, J. L. Guzmán, J. L. García Sánchez, J. L. Casas López, J. A. Sánchez Pérez

*Solar Energy Research Centre (CIESOL), Joint Centre University of Almeria - CIEMAT*
drg975@ual.es

## ABSTRACT

This work presents, for the first time, a control approach of the continuous flow operation of the solar photo-Fenton process in raceway pond reactors (RPR) designed for micropollutant (MP) removal from urban wastewater treatment plant (WWTP) secondary effluents. The control system was designed using the mechanistic and semiempirical kinetic model of the photo-Fenton process at acidic pH developed and validated in previous work. Afterwards, a simulation study to demonstrate the viability of the control system was conducted under different operating conditions (hydraulic residence time and liquid depth) for solar irradiance and water temperature variation over the year. Two liquid depths (10 and 20 cm) and two hydraulic residence times (15 and 30 min) were selected as operating conditions to study the system performance for different MP removal control setpoints (70 % and 90 %). The presented results demonstrate not only the feasibility of implementing an automatic approach for the solar photo-Fenton process, but also the need for an optimised, efficient and controlled operation to upgrade its competitiveness versus conventional technologies.

## METHODS

The control system was designed using the kinetic model of the solar photo-Fenton process at acidic pH, previously reported [1]. Therefore, two PI controllers were tuned applying classical methods to control MP and $H_2O_2$ concentration in the photoreactor by modifying $FeSO_4 \cdot 7H_2O$ and $H_2O_2$ feed flows ($Q_{Fe}$ and $Q_{H2O2}$, respectively). Then, a simulation study was conducted for different liquid depths (10 and 20 cm) and hydraulic residence times (15 and 30 min) for a solar photo-Fenton RPR operated in continuous flow mode, assuming perfect-mixing hypothesis. Note that actual data of the process was used (UV irradiance and temperature log records and water matrix composition) to faithfully reproduce the photo-Fenton plant. The control system performance was evaluated using the cost efficiency, which is a parameter that relates the mass of MP removed per unit of reactor surface area and monetary unit (mg $\cdot$ m$^{-2}$ $\cdot$ €$^{-1}$). Further information can be found elsewhere [2].

## RESULTS AND DISCUSSION

**Fig. 1** shows a one-day plant simulation (1 June 2021, Almería, Spain) for a cloudy operating day to show the disturbance rejection capabilities of the proposed control approach. At midday (12:00–15:00) the regular operation of the photo-reactor is strongly disturbed by an abrupt and intense cloud (**Fig. 1.a**). Consequently, the incident solar UV radiation is sharply reduced by 89 %, giving rise to an increase in MP concentration of up to 172 % for manual or open-loop (OL) operation (**Fig. 1.b**). However, for the automatic or closed-loop (CL) operation, the controller rapidly increases iron concentration in the reactor (**Fig. 1.d**) by modifying $Q_{Fe}$ (**Fig.

**1.c**) in order to cancel the system disturbance by compensating the decontamination through the Fenton reaction. As a result, MP concentration remains almost unchanged based on the control setpoint (**Fig. 1.b**), proving the robustness and effectiveness of the control system for disturbance rejection. Note that this is a very important advantage to ensure autonomous operation for these type of processes based on renewable energy sources.
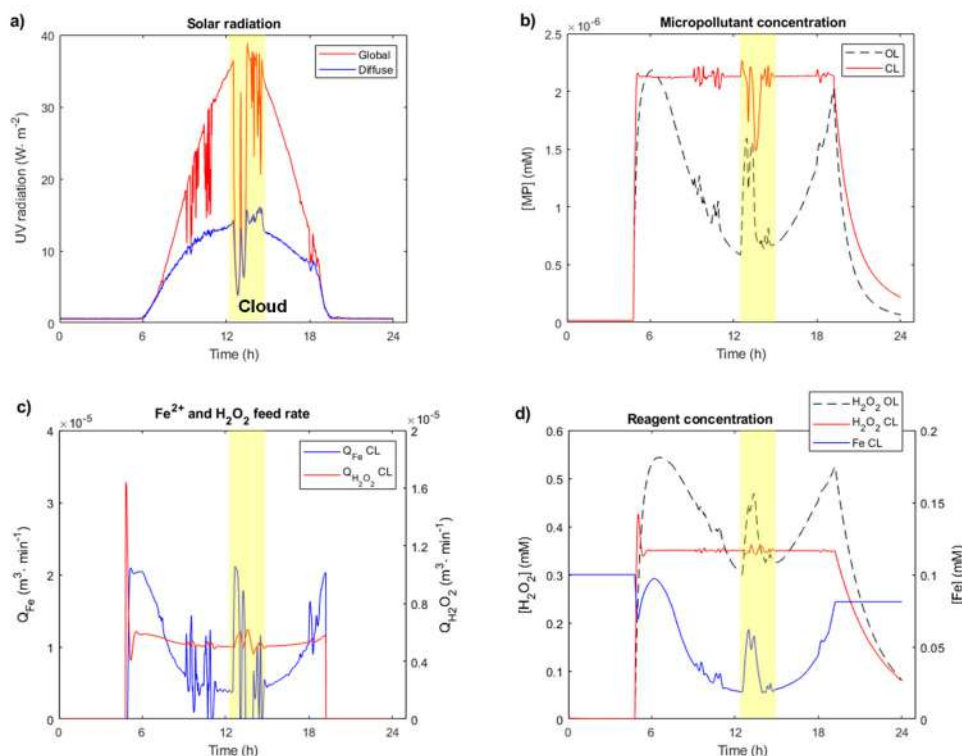


**Fig. 5.** Plant simulation for a cloudy operating day (1 June 2021, Almería, Spain). Global and diffuse UV solar radiation (a), MP concentration profile (b), $H_2O_2$ and $Fe^{2+}$ feed rates (c) and reagent concentration (d).

## CONCLUSIONS

This work contributes to achieving an automatic operation approach of the solar photo-Fenton process to improve the cost efficiency by maximising the use of solar radiation in the decontamination reaction. It can be concluded that highly demanding MP removal setpoints are achieved through high non-linear reagent consumption, resulting in low process operating cost efficiencies. In this way, the proposed control approach provides a free tuning parameter that can be used to look for a trade-off between performance and running costs. Consequently, other works have emerged focused on control setpoints optimization based on techno-economic criteria according to the environmental conditions.

## ACKNOWLEDGEMENTS

## REFERENCES

[**1**] J.A. Sánchez Pérez, S. Arzate, P. Soriano-Molina, J.L. García Sánchez, J.L. Casas López, P. Plaza-Bolaños, Science of the Total Environment, 736 (2020) 139681.

[**2**] D. Rodríguez-García, P. Soriano-Molina, J.L. Guzmán, J.L. García Sánchez, J.L. Casas López, J.A. Sánchez Pérez, Chemical Engineering Journal, 455 (2023) 140760.

# Thermochemical oxygen pumps: A promising candidate to increase the efficiency of thermochemical fuel production

Jens Keller[1,2], Mathias Pein[1], Nicole Neumann[1], Stefan Brendelberger[1], Christian Sattler[1,2]

[1]*Institute of Future Fuels, German Aerospace Center,*

[2]*RWTH Aachen, Chair for Solar Fuel Production*
Jens.Keller@dlr.de

The thermochemical fuel production process is one of the most promising methods to convert solar energy into green hydrogen or syngas. The high temperature heat required for the underlying redox cycle is supplied by concentrated solar energy with the principal ability to utilize the whole solar spectrum and is carried out in cyclic two-step process. In a reduction step the heat is used to endothermally reduce a metal oxide at high temperatures. In a temperature swing the pre-reduced metal oxide is cooled down to lower temperature and exothermally re-oxidized by reacting with water/steam or carbon dioxide to form hydrogen and/or carbon monoxide. [1]

State-of-the-art materials for this process such as Ceria are hard to reduce even at the high temperatures employed. In order to increase the reduction extent during the reduction step, and thereby the cyclic yield of the process, it is necessary to provide a controlled reducing atmosphere with a low oxygen partial pressure. While conventional vacuum pumping remains to be the state-of-the-art, alternative methods such as thermochemical oxygen pumping (TCOP) exhibit great potential to increase the efficiency of the fuel production process with comparatively little energy consumption. [2] With TCOP a second two step thermochemical cycle is employed to reduce the oxygen partial pressure during the reduction step. [5]

In comparison to conventional vacuum pumps, a TCOP only requires up to 90% less energy in a pressure range below 1 mbar and therefore has the ability to increase the overall efficiency of the thermochemical fuel production. This pumping process also utilizes redox metal oxides, which can be cycled at much lower temperatures than the splitting materials like Ceria. [3] Additionally, no mechanical components are required and recuperated heat from the thermochemical splitting cycle can be utilized to power the pumping cycle. [2]

The functional principle is shown in the graph below.
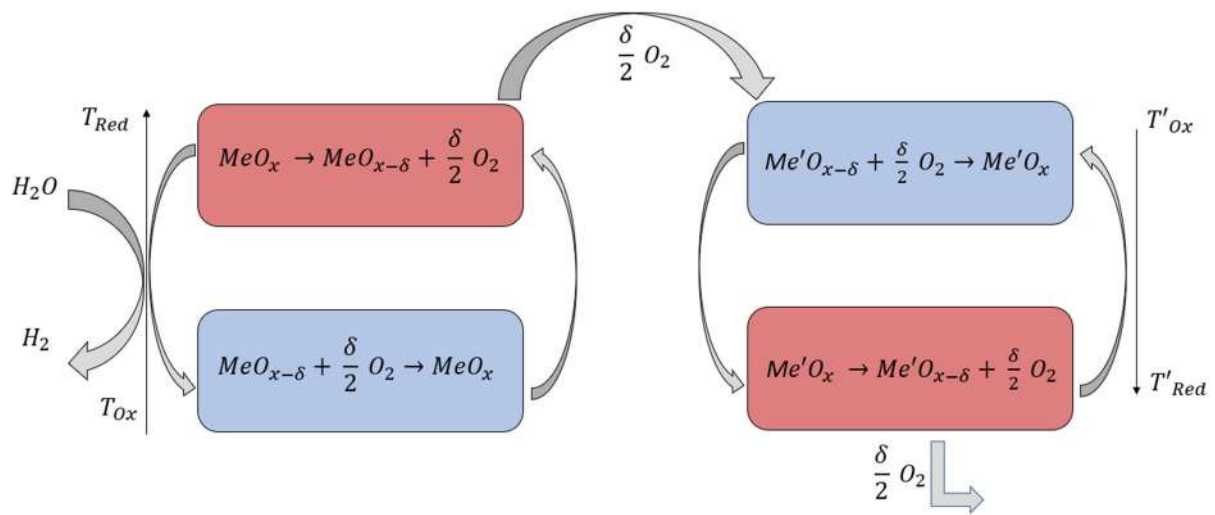
*Figure 3: Functional principle of a two-step thermochemical cycle for splitting water in combination with a two-step thermochemical cycle to provide a reducing atmosphere during the reduction step of the thermochemical splitting cycle.*

A proof of concept of this TCOP process has already been demonstrated [2,3], and efforts were made to identify suitable potent TCOP pumping materials. [4]

Proper modelling of various operational modes as well as simulation of practical scale-up scenarios of TCOP is crucial in order to identify optimized operational parameters and suitable pumping materials. As part of ongoing work, a sophisticated modelling approach is outlined in this work and initial results are discussed in the context of solar fuel production.

**[1]** Y. Lu et al., <u>Progress in Energy and Combustion Science</u>, 75, 2019, 100785

**[2]** S. Brendelberger et al., <u>Solar Energy</u>, 2017, 91-102

**[3]** M. Pein et al., <u>Solar Energy</u>, 2020, 612-622

**[4]** J. Vieten, <u>Energy Environ. Sci.</u>, 2019, 1369-1384

**[5]** B. Bulfin, <u>Energy Fuels,</u> 2015, 1001−1009

# Hydrogen production improvements byglycerol photoreforming under natural radiation at pilot scale

J. G. Villachica Llamosas [1], A. Ruiz-Aguirre[1], S. Malato[1].

*(1) CIEMAT – Plataforma Solar de Almería, Ctra. De Senés s/n, 04200 Tabernas, Almería, Spain.*
*jgvillachica@psa.es.*

Climate change and environmental degradation, due to carbon-based fossil fuels for energy production, has increased. In this sense, renewable energy resources are being developed and promoted. To support EU's commitment, the replacement of the use of fossil fuel to produce energy into renewable energy, is expected to be achieved by 2050, thanks to the implementation of the European Green Deal and the New Green Deal in United States plans, [1]. Hydrogen, as feedstock, fuel and energy carrier, is gaining attention; however, is still largely produced from fossil fuel ($CH_4$ and CO steam reforming) or from electrolysis using electricity from fossil fuels. A suitable and renewable (or clean) alternative is hydrogen produced by photocatalytic water splitting (heterogeneous photocatalysis), which should achieve a solar-to-hydrogen (STH) energy conversion efficiency of 5-10% to be economically viable. Nevertheless, currently, STH values are around 1% for water splitting at laboratory scale [2]. For that, the research in this field is focused on finding the photocatalyst, the operating conditions and the design of the photoreactor that allow to increase the efficiency up to competitive values. One approach has been the use of sacrificial agents (organic electron donors), as glycerol, an abundant byproduct of biodiesel wastewater that allows wastewater revalorization [3]. To evaluate the viability of this technology, different photocatalysts and operating conditions has been tested in this PhD Thesis, trying to findthose that result in the highest efficiency with a stable photocatalyts.

Among the main objectives of the PhD already showed in former SOLLAB Doctoral Colloquiums, have been presented studies of glycerol photoreforming in different water matrixes (demineralized water and natural water) at pilot scale, tested with different photocatalysts: 1) physical mixture of $TiO_2$ with CuO or NiO; 2) synthesized photocatalysts as $gC_3N_4$-urea, $gC_3N_4$-urea- CuO, $gC_3N_4$-melamine, $gC_3N_4$-Ru and C-Ru; 3) soft calcination of photocatalyst at different temperatures (200-400 °C) and times (1-6 h) [4]; 4) simultaneous $H_2$ production with the elimination of a recalcitrant organic contaminant imidacloprid (180 min) and a standard water pathogen *Escherichia coli* disinfection (10 min) [3].

The last step of the PhD consisted of studying different natural water (NW) qualities (NW1=1.4 mS·cm$^{-1}$, NW2= 0.72 mS·cm$^{-1}$, NW3=0.47 mS·cm$^{-1}$) with the mixture NiO:TiO$_2$ (1:10) in different concentrations (50 mg·L$^{-1}$, 100 mg·L$^{-1}$, 200 mg·L$^{-1}$). Results showed that the presence of salts in natural water, reduced process efficiency requiring a higher concentration of photocatalyst (Fig.1). Finally, a ternary photocatalyst was tested with glycerol (0.075M) in demineralized water. The physical mixtures were composed of TiO$_2$ with CuO and NiO in different ratios for three different percentages of total metal (5%, 7.2% and 10%) for a concentration of the ternary photocatalyst of 100 mg·L$^{-1}$. The best results were obtained for a percentage of metal of 7.2 % with the same quantity of each metal, resulting in a STH of 1.71 % (Fig. 2).
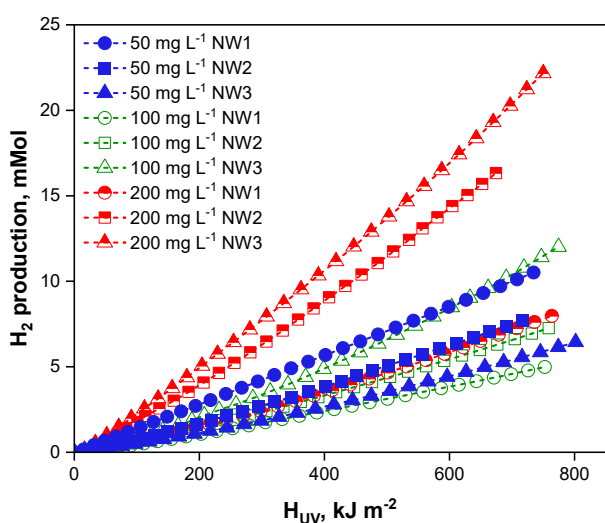


**Fig 1.** H$_2$ production in natural water with NiO:TiO$_2$.　　**Fig 2.** Photocatalytic H$_2$ generation with CuO :NiO :TiO$_2$
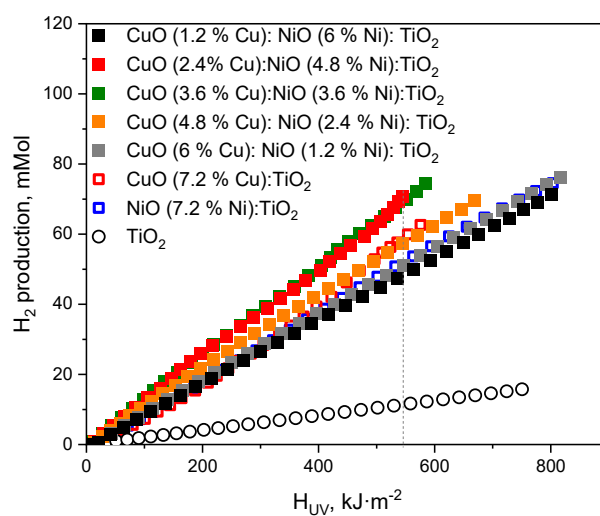
**[1]** European Union: European Comission, communication from the commission to the european parliament, the council, the european economic and social committee and the committee of the regions, Brussel, 8.7.2020, COM (2020) 301-end, https://eur-lex.europa.eu/legal-content/EN/TXT/?uri=CELEX:52020DC0301.

**[2]** Z. Wang, C.Li, K. Domen. Chem. Soc. Rev. 48 (2019) 2109-2125.

**[3]** A. Ruiz-Aguirre, J.G. Villachica-Llamosas, M.I. Polo-López, A. Cabrera-Reina, G. Colon, J. Peral, S. Malato. Energy 260 (2022), 125199.

**[4]** J. G. Villachica-Llamosas, A. Ruiz-Aguirre, G. Colón, J. Peral, S. Malato. International Journal of Hydrogen Energy, in press, 2023.

# Development of a thermally coupled photoelectrochemical system for water splitting under concentrated sunlight

Elisa Gruber[1,2], Michael Wullenkord[1], Christian Sattler[1,2]

[1]*German Aerospace Center (DLR), Institute of Future Fuels*
[2]*RWTH Aachen University, Chair for Solar Fuel Production, Aachen, Germany*
*Elisa.Gruber@dlr.de*

Hydrogen is a versatile chemical required for many industrial processes. In light of the global efforts to reduce fossil fuel usage, it is also steadily gaining relevance as an energy storage and fuel. Integrated photoelectrochemical (PEC) systems, which combine photovoltaic (PV) cells for electricity production with electrolyser cells (ECs) for water splitting, offer a promising carbon-neutral way of producing hydrogen from solar energy. When combined with optical concentrators, PEC systems become particularly compact and efficient, as this increase in irradiation allows for the use of smaller PV cells, and hence more expensive semiconductor materials [1,2].

Higher solar-to-hydrogen efficiencies can be achieved when the PV cell and the water electrolyser are not just electrically, but also thermally coupled [1]. While PV cells work best at ambient temperatures, the ideal operating temperatures of an EC are somewhat higher (depending on the exact type). By coupling both components thermally, the heat that is generated in the concentrated photovoltaic (CPV) cell as an undesired by-product can be diverted to the EC and elevate it to higher temperatures, which lead to lower overpotentials [1].

Despite this beneficial thermal exchange between CPV cell and EC, such concentrated PEC systems still require active cooling due to the high irradiation they are exposed to and the fact that most commercial water electrolysers are designed to operate above their thermoneutral voltage, where they too generate excess heat. To recover this waste heat the presented work incorporates a thermally coupled process (TCP) as a third pillar of the overall system. The goal of this is to utilise as much of the electrical and thermal energy provided by the CPV unit as possible, while maximising the solar-to-hydrogen efficiency. To find the most suitable combination of CPV cell, EC and TCP, a literature research was conducted, which determined a wide variety of options for each of them:

It is a general consensus amongst solar researchers that multijunction cells are the best choice for CPV applications, especially when applied in point-focused systems, which can reach particularly high concentrations [2]. The PEC system developed in this work however, is intended for use in linear concentrators such as parabolic troughs, which are easily scalable and limited to a concentration of about 100 Suns. At these concentrations, modern silicon PV cell concepts such as Si-heterojunctions are also viable options [3].

There are five suitable types of EC that can be categorized into low- and high-temperature cells. Low-temperature water electrolysis at temperatures below 150 °C can be performed by an alkaline EC, a proton exchange membrane (PEM) EC or an anion exchange membrane (AEM) EC. In the high-temperature category operating above 400 °C proton-conducting (PC) ECs and oxygen-ion-conducting solid oxide (O-SO) ECs come into play.

Two kinds of TCP are being considered for the coupled PEC system: (A) processes that transform heat into further electricity to power the EC, such as Organic Rankine Cycles (ORC) and thermoelectric generator (TEG); and (B) processes generating steam.

By taking into account the boundary conditions of the different components, especially their temperature sensitivities and required heat flows, first combinations of CPV cell, EC and TCP were assembled into innovative solar-to-hydrogen systems. From this selection three types of promising thermally coupled PEC systems can be defined: (1) systems in which the TCP is positioned downstream of an integrated PV-EC unit; (2) systems in which a TCP of type B is located between a PV cell and a high-temperature EC; (3) systems involving a beam splitter that directs only the part of the solar spectrum onto the CPV cell, which aligns with the spectral response of the latter, leaving the remainder of the irradiation for thermal use.

In conclusion, thermally coupled PEC systems seem to have the potential of being a particularly efficient and compact solar-to-hydrogen path. To show this, the systems defined in the presented work will be assessed and narrowed down based on several selection criteria, such as overall efficiency, cost-effectiveness, technology readiness and use of earth-abundant materials. The most promising system will then be modelled in more detail and tested at demonstration scale using DLR's solar testing facilities.

[1] I. Holmes-Gentle, S. Tembhurne, C. Suter, S. Haussener, Nat Energy, 8 (2023) 586-596.

[2] I. Rey-Stolle, J.M. Olson, C. Algora, in *Handbook of Concentrator Photovoltaic Technology*, I. Rey-Stolle, C. Algora (Eds.), United Kingdom, Wiley, 2016, 59-116.

[3] A. Descoeudres, C. Allebé, N. Badel, L. Barraud, J. Champliaud, F. Debrot, A. Faes et al. Energy Procedia, 77 (2015) 508-514.

# Development and Investigation of a Reactive Heat Exchanger

Anika Weber[1,2], Johannes Grobbel[1], Christian Sattler[1,2]

*[1]German Aerospace Center (DLR), Institute for Future Fuels*
*[2]RWTH Aachen, Chair for Solar Fuel Production*

*Anika.Weber@dlr.de*

Carbon neutral production of hydrogen is one promising path to achieve the target of $CO_2$ neutrality by 2050. Besides the most common way of electrolysis driven by renewable energy, one way of green hydrogen production is the utilization of a thermochemical redox cycle.

In this cycle, a redox material is firstly endothermically reduced under the release of oxygen at high temperatures (at more than $1400\,°C$) and low oxygen partial pressures (approximately below $120\,Pa$). High temperatures can be reached by concentrated solar radiation which utilizes all wavelengths of the sunlight. CSP can be provided by a heliostat field that reaches concentration factors as high as $3000$. Low oxygen partial pressures can be obtained by vacuum technology, sweep gas or a combination of both. [1]

In a second step, the redox material is re-oxidized at significantly lower temperatures around $900°C$. Using water vapor as oxidizer, hydrogen is created. It is also possible to use a mixture of carbon dioxide and steam as oxidizer to create synthetic gas, which can be converted to kerosene using a Fischer-Tropsch process. After oxidation, the redox material can be reused for the reduction process. [1]

Several reactor concepts have been demonstrated and presented so far. One of them is a novel sweep gas and particle-based concept called *SOMPIHR (Sweeped, Open, Moving Particle reactor Including Heat Recovery)* [3]. A steady state analysis indicates promising solar-to-fuel efficiencies as high as 18 % [3].

In this concept, a crucial component is a reactive, direct contact, moving bed heat exchanger called RedHX. In the RedHX, the particles are reduced by a countercurrent sweep gas. Several, partly competing requirements exists for the design and realization of the RedHX. One of these requirements is the need for a shallow bed which also supports a homogeneous sweep gas flow. In order to demonstrate the feasibility, the RedHX developed and investigated further in an experimental campaign and in a detailed CFD-DEM model.

**[1]** C. Agrafiotis, M. Roeb, C. Sattler, in *Comprehensive Energy Systems vol. 4*, I. Dincer (Eds.), Netherlands, Elsevier, 2018.

**[2]** S. Zoller, E. Koepf, P. Roos, A. Steinfeld, J. Sol. Energy Eng., 141 (2) (2019) 021014

**[3]** A. Weber, J. Grobbel, M. Neises-von Puttkamer, C. Sattler, J. Sol. Energy (2023) submitted.

# Modeling the CeO$_2$-CH$_4$-CO$_2$ Redox Reforming Cycle in OpenFOAM

Mario Zuber, Simon Ackermann, Aldo Steinfeld

[1]Department of Mechanical and Process Engineering, ETH Zurich, Switzerland
mazuber@ethz.ch

[2]Synhelion SA, Switzerland

Thermochemical processes using concentrated solar energy as the source of high-temperature heat offer an efficient pathway for producing sustainable fuels. A precursor to these liquid fuels is syngas (H$_2$ and CO), which can be produced via dry reforming of CH$_4$ with CO$_2$.

Within this framework CeO$_2$ is introduced as an active redox material over which dry reforming can occur. Dry redox reforming is represented by:

reduction: $\mathrm{CeO_2} + \delta\mathrm{CH_4} \rightarrow \mathrm{CeO_{2-\delta}} + \delta\mathrm{CO} + 2\delta\mathrm{H_2}$

oxidation: $\mathrm{CeO_{2-\delta}} + \delta\mathrm{CO_2} \rightarrow \mathrm{CeO_2} + \delta\mathrm{CO}$
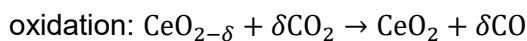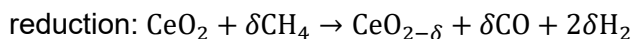
$\delta$ represents the non-stoichiometry of CeO$_2$. The process operates isobarically and isothermally at around 1000°C. The use of a redox material avoids the use of a catalyst, avoids unwanted products (e.g. C(s)), and serves as an interim technology preceding the solar-driven production of syngas from H$_2$O and CO$_2$ which operates at higher temperatures (1500°C).

We report on the implementation of the thermodynamics into a computational fluid dynamic model using a customized solver in OpenFOAM (an open-source CFD software package). The solver considers the mass and energy conservation equations in both the gas and solid phase, and notably allows to model reversible heterogenous reactions of a non-stoichiometric metal oxide. A tubular reactor ($\varnothing$=19 mm, l=200 mm) filled with a packed bed of CeO$_2$ pellets is used to validate the model. Main operating conditions include mass flowrates of 1L/min (L:normal liters), 1000°C, and up to 5% reactive gas concentrations.

# 3D-Printed Ceria Structures for Enhanced Radiative Heat Transfer of Concentrated Solar Energy

Sebastian Sas Brunser[1], Hugo Braun[1], Lukas Schlagenhauf[1], Fabio Bargardi[2], Rafael Libanori[2], André R. Studart[2], and Aldo Steinfeld[1]

[1]ETH Zürich, Department of Mechanical and Process Engineering, 8092 Zurich, Switzerland

[2]ETH Zürich, Department of Materials, 8093 Zurich, Switzerland
sasbrunser@ethz.ch

We report on the printing and testing of novel porous ceria structures for $CO_2$ splitting via a redox thermochemical cycle driven by concentrated solar energy. These structures were 3D-printed using a Direct Ink Writing (DIW) technique and were designed with hierarchically ordered porosity gradients to circumvent Beer-Lambert's exponential attenuation law and thus enable longer propagation of the incoming radiation [1]. Experimental testing was performed in a solar-driven thermogravimetric analyzer, in which the ceria samples were directly exposed to high-flux irradiation, mimicking the realistic operation of solar reactors. Their mass change, temperature, and product gas composition were continuously monitored during the redox reactions. Temperatures and reaction extents were compared with those obtained with a reticulated porous ceramic (RPC) structure with equal volume, serving as the state-of-the-art reference. Remarkably, the 3D-printed structures achieved a higher and more uniform temperature profile than the RPC, doubling the CO yield. Stability was confirmed for vacuum-coated 3D-printed samples by performing 100 rapid-temperature cycles in an IR furnace.

[1]     Sas Brunser, S., et al., Advanced Materials Interface, 2023.

# Development of a Redox Material Assembly for Solar Thermochemical Fuel Production

Louis Thomas[1], Stefan Brendelberger[1], Christian Sattler[1,2]

*1.German Aerospace Center (DLR), Institute of Future Fuels*

*louis.thomas@dlr.de*

*2.RWTH Aachen, Chair for Solar Fuel Production*

With a two-step thermochemical reduction-oxidation (redox) cycle, it is possible to produce $H_2$ and $CO$ via $H_2O$ and $CO_2$ splitting respectively. If concentrated solar radiation is used as energy input, e.g. via a heliostat field, this process is capable of producing solar fuels (e.g. kerosene) [1]. In order to make this approach an economical feasible pathway for the large-scale production of sustainable fuels, further developments of the solar reactors and splitting materials are necessary.

The first endothermic step of the cycle reduces a redox material (e.g. CeO$_2$) at high temperatures ($T_{red} \geq 1400\,°C$) and low oxygen partial pressures ($p_{O_2} \sim 1\,mbar$). Concentrated solar radiation can provide the energy necessary for reaching the high temperatures and thereby releasing oxygen from the redox material. In a second oxidation step $H_2O\,/\,CO_2$ is brought into contact with the reduced material at lower temperatures ($T_{ox} \leq 1000\,°C$). The redox material is now capable of splitting oxygen apart and producing $H_2\,/\,CO$ respectively, while re-oxidizing to its initial state which allows a cycling operation.

The current state-of-the-art reactor design works in a batch operation mode, where the entire reactor needs to be cycled between the reduction and oxidation temperature. This temperature swing operation consumes a large fraction of the energy input and takes time. Furthermore, the redox material is not homogeneously heated, but rather exhibits high temperatures at the directly irradiated front and much lower temperatures at the back. This results in a non-uniform reduction extent along the material thickness and limits the overall splitting potential.

In order to address these challenges and improve the overall process efficiency, a novel reactor concept (R2Mx) is proposed. The R2Mx design separates the reactor into two distinct chambers for the reduction and oxidation step [2]. The redox material is mounted on top of a transport unit in order to move the material between the reduction and oxidation chamber. The redox material in combination with an insulating connector and the mounting is a novel

component, called redox material assembly (RMA). The cyclic operated process defines the boundary conditions for which the RMA has to be developed.

For the optimization of the design and operation of such an RMA, a numerical model will be developed. The model simulates heat transfer, fluid dynamics and redox reactions with changing boundary conditions representing the changing reactor environments during cyclic operation. Currently the R2Mx proof-of-concept test rig is under development, which will be used to test RMA units and to provide data for model validation. The modelling approach and some initial results will be presented.

[1] S. Zoller, E. Koepf, D. Nizamian, M. Stephan, A. Patané, P. Haueter, M. Romero, J. González-Aguilar, D. Lieftink, E. de Wit, S. Brendelberger, A. Sizmann, and A. Steinfeld, Joule 6, 1606 (2022) 1606–1616.

[2] S. Brendelberger, P. Holzemer-Zerhusen, E. Vega Puga, M. Roeb, and C. Sattler, Solar Energy 235, 118 (2022) 118–128.

# Concentrating solar thermal synthesis of C12A7:e⁻ electrides, a photothermal catalyst for solar fuels production

Ehsan Hajialilou, Laura Collado, Manuel Romero, Víctor A. de la Peña O'Shea, José González.

*IMDEA Energy*
jose.gonzalez@imdea.org

Electrides are intriguing candidates for industrial uses, of which interest has grown during the past few years. In essence, an electride is a special family of quantum materials in which extra electrons are trapped inside crystal cavities acting as anions. These materials have a range of special features that make them appealing for use in many different catalytic and electron emission applications. Over the last decade, significant efforts have been dedicated to investigating alternative inorganic substitutes for organic electrides at room temperature (RT). This is primarily due to the limited thermal and chemical stability of organic electrides. Consequently, there is a strong focus on actively pursuing cost-effective and environmentally sustainable synthesis methods for these materials.

Mayenite, a calcium aluminate with the chemical formula $12CaO_7Al_2O_3$ (known as (C12A7:e⁻), is an electride which crystal structure consists of one positively charged lattice framework containing 12 sub-nanometre cages and four clathrates electrons (e⁻) randomly accommodated in 4 out of 12 cages (see Figure 1). Mayenite has particularly remarkable behaviour under many experimental conditions because it can store extra oxygen ions in its nanocages.
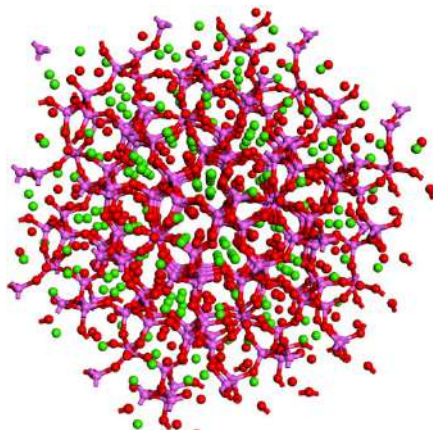


Figure 1. Crystal structure of mayenite, $Ca_{12}Al_{14}O_{33}$.

Mayenite synthesis requires that the precursor materials react at high temperatures (about 1450 °C) in a nitrogen atmosphere to promote crystallization and ensure the integrity and purity of the material, which is usually performed in high-temperature furnaces. This works analyses the feasibility of synthesizing C12A7: e⁻ using concentrated light by means of a high-flux solar simulator (HFSS) (Figure 2), as a preliminary step towards an environmentally friendly alternative for mayenite production based on concentrated solar energy.

In this work, the precursors are directly irradiated by concentrated light and consequently, temperature distribution and heating rates differ from those of the high-T furnace. By conducting a comparative analysis of outcomes from the furnace and the HFSS, we aim to identify the most effective and sustainable approach for synthesizing high-quality C12A7:e⁻. Consideration of factors such as crystallinity, morphology, and optical properties is essential for its potential application in photothermal processes. X-ray diffraction (XRD) is used to determine the crystal structure, phase purity, and crystallinity, which provides insights into the arrangement of atoms within the crystal lattice and confirms the formation of C12A7:e⁻ electride. Scanning electron microscopy (SEM) and transmission electron microscopy (TEM) are used to study the surface morphology and microstructure of the material at both the macroscopic and nanoscale levels, providing insights into the size, shape, and distribution of the particles as well as the presence of internal defects and interfaces. In addition, the optical properties will be investigated using UV-Vis spectroscopy and photoluminescence spectroscopy to evaluate the material's ability to absorb and emit light.
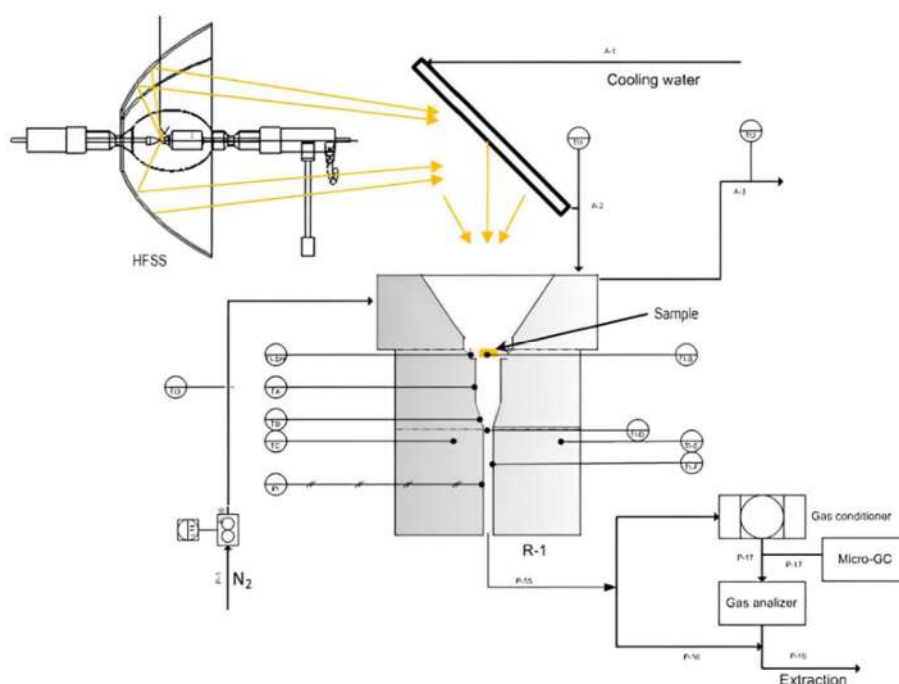


Figure 2. Scheme of the high-flux solar simulator for the mayenite synthesis.

# Thermogravimetric study of Sr- and Al-based metal nitrides for the thermochemical production of ammonia

Daniel Notter[1], María-Elena Gálvez[2], Brendan Bulfin[1], Carlos Triana[3], Greta R. Patzke[3], Aldo Steinfeld[1].

[1] *Department of Mechanical and Process Engineering, ETH Zurich, 8092 Zurich, Switzerland.*
*danotter@ethz.ch*

[2] *Instituto de Nanociencia y Materiales de Aragón, Universidad de Zaragoza, 50018, Zaragoza, Spain.*

[3] *Department of Chemistry, University of Zurich, 8057 Zurich, Switzerland.*

Industrially produced ammonia ($NH_3$) via the Haber-Bosch process consumes approximately up to 2% of the total global energy generated and is responsible for $CO_2$ emissions in the same order of magnitude. A growing population and increasing interest in $NH_3$ as a fuel or $H_2$ carrier ensure a continuing demand for it. Thus, exploring alternative $NH_3$ production routes becomes critical for reducing the overall anthropogenic $CO_2$ footprint. One promising alternative is a two-step thermochemical cycle based on metal nitrides, consisting of: 1) a high-temperature endothermic nitridation step driven by concentrated solar energy, followed by 2) a low-temperature exothermic hydrogenation step for the synthesis of $NH_3$.

The thermochemical cycle is experimentally demonstrated using Sr-based and Al-based metal nitrides. We perform rigorous mass balances for both steps of the cycle using a thermogravimetric analyzer, supplemented by a $NH_3$ UV photometer gas analyzer, an $H_2$ thermal conductivity gas analyzer, and a mass spectrometer. For further characterization, the compositions of the solid phases are determined by X-ray diffraction.

# Development of a High-Temperature Counter-Flow Particle Receiver for Concentrated Solar Power Applications

Anton Hartner[1], Filippo Coletti[1] & Aldo Steinfeld[1]

[1]*Department of Mechanical and Process Engineering, ETH Zurich, 8092 Zurich, Switzerland*
*ahartner@ethz.ch*

In concentrated solar power (CSP) plants, solar radiation is concentrated onto a solar receiver and absorbed as high-temperature heat in a heat transfer medium. Using a particle-flow as the heat transfer medium allows for outlet temperature exceeding 1000°C and for simultaneous thermal energy storage by collecting the hot particles downstream in an insulated silo. Controlling the residence time of the particles during direct high-flux irradiation is critical because it has a direct effect on their exit temperature[1]. Here, a solar particle receiver is designed to enable controllability of the residence time. It consists of a cavity-receiver containing a vertical ceramic duct through which particles are falling against a counter-current flow of air. A 1D two-phase heat transfer model of the duct is developed to investigate the influence of different solid volume fractions and particle sizes. For a given solid volume fraction, smaller particles enhance heat transfer but at the same time make them more difficult to handle. Ceramic particles ranging between 200 and 300 μm were found to be appropriate for the present design. In order to investigate how effectively the residence time of the particles can be controlled, a facility with transparent test section and a 20 mm × 20 mm cross-sectional area was designed and built that allows the hydrodynamics of the particle-laden flow to be studied with high-speed imaging under room temperature conditions. The facility enables to vary the solid volume fraction inside the duct from 0.1% to 10%. The 1D heat transfer model captures that for a constant solar cavity temperature, the particle outlet temperature decreases as the solid volume fraction increases. For solid volume fractions between 0.1% and 1% and a solar cavity temperature of 1527°C, the model predicts that particle outlet temperatures above 1000°C can be achieved.

[1] C. K. Ho, Applied Thermal Engineering, 109 (2016) 958-969.

# Evaluation of the efficiency and pressure drop in metallic wire meshes with stagger pattern for solar tower technology

Daniel Sanchez-Señoran[1], Michael P. Kinzel[2], Miguel A. Reyes-Belmonte[3], Antonio L. Avila-Marin[1]

[1] CIEMAT – Plataforma Solar de Almeria (PSA), Avda. Complutense 40, Madrid E-28040, Spain
[2] University of Central Florida (UCF), 4000 Central Florida Blvd, Orlando, FL 32816, United States of America
[3] Rey Juan Carlos University (ESCET), C/ Tulipan s/n, Mostoles-Madrid E-28933, Spain
daniel.sanchez@ciemat.es

## 1. Introduction

Open volumetric receivers (OVR) are one of the developing technologies for Concentrated Solar Tower (CST), in comparison with the current commercial plants, the OVR technology provides higher working temperatures and easier operation and maintenance. Air is used as the working fluid in this technology within the purpose of refrigerating the OVR causing the absorption of as much heat as possible for a later usage in heat processes or power cycles. Ceramic and metallic materials dominate the OVR technology exposing several examples like ceramic or metallic foams, metal wire meshes, so forth [1]. This study evaluates the thermal performance and pressure drop of an OVR made of metallic wire meshes following a staggered stack pattern with 80% fixed screen porosity based on different geometrical parameters, such as wire diameter (d) and wire spacing (w).

## 2. Numerical methodology

This study has adopted the commercial software STAR-CCM+ 18.02.008 with its feature Design manager for the development of the simulations following the validated numerical methodology [2]. It is determined by a simplified 2D model of 60 mm length and height which is used to solve the equations applied in the Porous Medium method with local thermal non-equilibrium (LTNE) state. Also, steady state, laminar flow, ideal gas and segregated fluid temperature and flow have been established in these simulations. The Rosseland approximation is followed in the radiative approach. A summary of the physic equations is presented [3]:

**Mass conservation and momentum equations**

$$\nabla(\rho_f \, v_D) = 0$$

$$\frac{1}{\varnothing^2}\nabla(\rho_f \, v_D \, v_D) = -\nabla\langle P_f\rangle^f + \frac{\mu_f}{\varnothing}\nabla^2 v_D - \left[\frac{\mu_f}{K_1} - \frac{\rho_f}{K_2}[\,v_D]\right]v_D$$

**Energy equations**

$$\nabla\left(\langle\rho_f \, c_{P_f} \, T_f\rangle^f v_D\right) = \nabla\left(k_{eff,f}\nabla\langle T_f\rangle^f\right) + h_v\left(\langle T_s\rangle^f - \langle T_f\rangle^f\right)$$

$$0 = \nabla\left(k_{eff,s}\nabla\langle T_s\rangle^s\right) + h_v\left(\langle T_f\rangle^s - \langle T_s\rangle^s\right) - S_{rad}$$

**Radiation approach**

Incident solar radiation
$$S_{rad} = \varepsilon \, a \, I_{z=0} \, e^{-\beta z}$$

Thermal radiation
$$q_{rad} = -k_{rad}\nabla\langle T_s\rangle^s$$

## 3. Results

In this work, staggered wire mesh stacks are presented with a wire diameter (d) variation from 0.1 to 0.7 mm, maintaining 80% fixed screen porosity [4]. These OVR have been evaluated under an inlet velocity range from 0.1 to 2 m/s, and an incident radiation variation from 300 to 1800 kW/m$^2$. The efficiency and the pressure drop in each OVR will be affected differently according to the established inlet velocity and incident radiation, for that reason an inlet velocity and incident radiation sweep are analyzed.

Fig. 4 depicts the pressure drop profile for each studied OVR under an inlet velocity range from 0.3 to 1 m/s and 600 kW/m$^2$. It is observed that larger wire diameter (d) and higher outlet fluid temperature leads to lower pressure drop, whereas, higher inlet velocity leads to higher pressure drop, showing a great absolute and relative pressure drop variation as function of the wire mesh diameter (d). **Error! Reference source not found.** shows the thermal efficiency of each OVR for an air inlet velocity between 0.3 and 1 m/s and an incident radiation of 600 kW/m$^2$. It is noteworthy that the OVR with a wire diameter of 0.4 mm has the best performance when inlet velocities are higher than 0.6 m/s with an outlet fluid temperature lower than 950K, however, higher wire diameters perform better when higher outlet fluid temperatures are aimed.
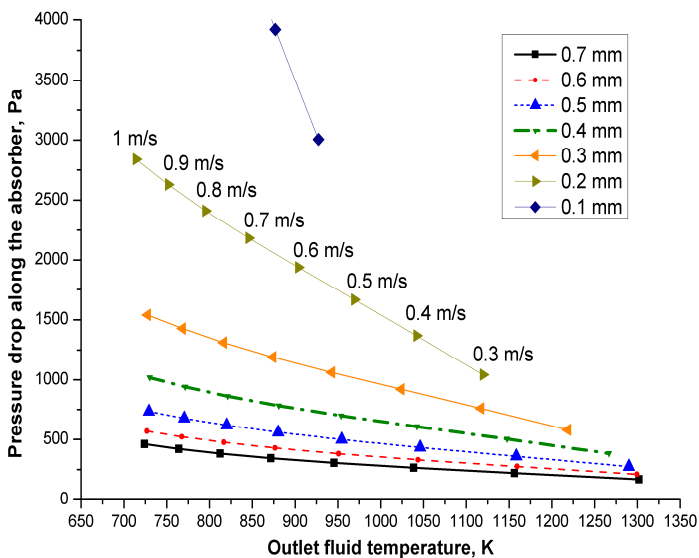


Fig. 4: Pressure drop profile against the outlet fluid temperature for each OVR wire diameter and inlet velocities from 0.3 to 1 m/s. Incident radiation is set to 600 kW/m$^2$.
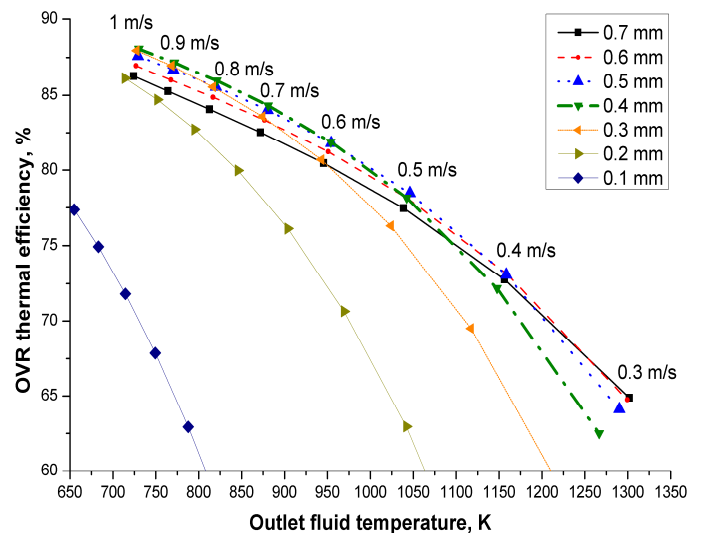
Fig. 5: OVR thermal efficiency against the air outlet temperature for each OVR wire diameter and inlet velocities from 0.3 to 1 m/s. Incident radiation is set to 600 kW/m$^2$.

## 4. References

**[1]**   Ávila-Marín AL. Sol Energy 2011; 85:891–910.

**[2]**   Avila-Marin AL et al. Renew Energy 2022; 201:256–72.

**[3]**   Avila-Marin AL et al. Renew Sustain Energy Rev 2019; 111:15–33.

**[4]**   Sanchez-Señoran D et al. Results Eng. 2023; 17:100830.

# Development of a nanofluid-based direct absorption parabolic trough solar collector using carbon nanoparticles

M. Sainz Manas [1,2,*], F. Bataille [1,2], C. Caliot [3], G. Flamant [1,*], and A. Vossier [1]

[1] Processes, Materials and Solar Energy Laboratory, PROMES - CNRS, UPVD, 7 rue du Four Solaire, 66120, Font-Romeu Odeillo.

[2] Processes, Materials and Solar Energy Laboratory, CNRS-UPVD, Perpignan University, Tecnosud, Rambla de la Thermodynamique, 66100 Perpignan, France

[3] Laboratory of Mathematics and its Applications, Université de Pau et des Pays de L'Adour, E2S UPPA, CNRS, LMAP, all´ee du parc Montaury, 64600, Anglet, France

*Corresponding authors: miguel.sainz-mana@promes.cnrs.fr , gilles.flamant@promes.cnrs.fr

Recent studies have demonstrated the potential of nanoparticles to enhance the optical and thermal properties of heat transfer fluids for direct absorption solar collectors (DASC) (**Figure 1**) [1–3]. In a DASC, the transfer fluid absorbs volumetrically the incident radiation, resulting in a more homogeneous fluid temperature distribution and less heat losses than in conventional surface collectors. The optical absorption in the visible range (300 – 900 nm) of conventional heat transfer fluids (HTF) is low. By using nanofluids incorporating a small volume fraction of nanoparticles, between 0.001 % and 1 %, the optical absorption in the visible range can be selectively increased. Nanofluid-based DASC (NDASC) have proved their potential to compete with both concentrating and non-concentrating solar thermal collectors, [1,4]. Water and thermal oils are commonly selected as base fluids, inside which metal, metal-oxides, or carbon nanoparticles are dispersed. Special attention has been given to carbon nanoparticles owing to their interesting optical and thermal properties as well as their low corrosion compared to metal or oxide nanoparticles. Carbon nanotubes as well as graphite nanoparticles have been widely studied for NDASC applications, but investigations related to graphene-based nanofluids for NDASC remain scarce [5–8]. Few experimental studies of concentrating NDASC are found in the literature and, to the authors knowledge, no experimental studies of graphene-based parabolic-trough NDASC have been done.
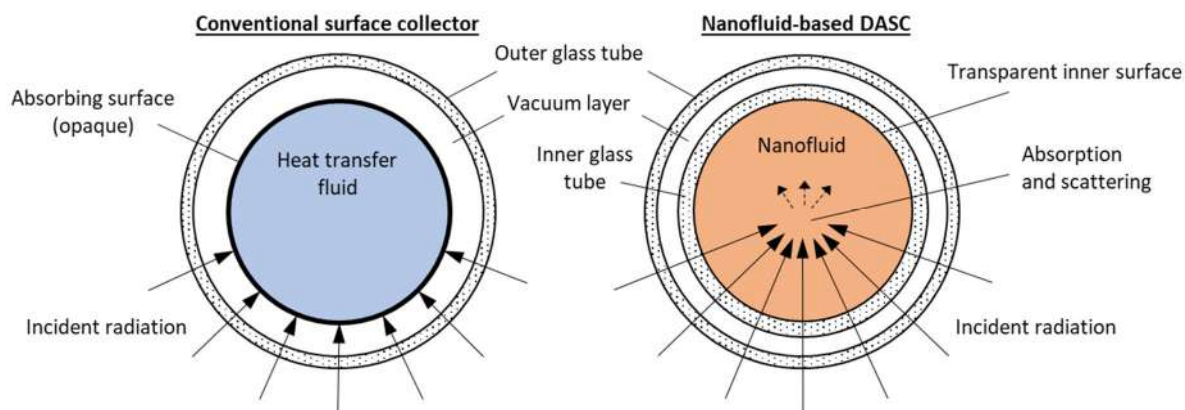
***Figure 1****: Schematic representation of the optical principle of a conventional tubular surface collector and a nanofluid-based tubular DASC.*

In this work, graphene nanoparticles dispersed in demineralized water are studied numerically and experimentally for a parabolic trough NDASC. First, the nanofluid spectral optical properties have been characterized, and transmittance values of 20 % and 5 % have been measured on 0.0044 % and 0.0088 % volume fraction of nanoparticle respectively (for a 50 mm fluid depth). Stability tests didn't show any sedimentation of the graphene nanoparticles after several months at room temperature (293 K), nor after being heated at 353K for 96 hours. The thermal conductivity of the base fluid is slightly enhanced by the nanoparticle addition but remains negligible, similarly to other thermo-physical properties of the base fluid as viscosity or density. These results confirm the potential of the nanofluid for concentrating NDASC applications.

An experimental parabolic-trough NDASC has been constructed to evaluate the performance of this kind of collector and analyze the influence of different parameters such as the receiver diameter, flow velocity and nanoparticle concentration. A numerical model is being developed to study the solar radiation absorption of the nanofluid in a concentrating NDASC (ray-tracing model) as well as the fluid flow and the temperature elevation of the nanofluid flowing in a 2 m-long absorber tube.

## **REFERENCES**

[1] Otanicar TP, Phelan PE, Prasher RS, Rosengarten G, Taylor RA., Journal of Renewable and Sustainable Energy, 2 (2010) 033102.
[2] Taylor RA, Phelan PE, Otanicar TP, Adrian R, Prasher R., Nanoscale Res Lett, 6 (2011) 225.
[3] Sainz-Mañas M, Bataille F, Caliot C, Vossier A, Flamant G., Energy, 260 (2022) 124916.
[4] O'Keeffe GJ, Mitchell SL, Myers TG, Cregan V., International Journal of Heat and Mass Transfer, 126 (2018) 613–624.
[5] Liu J, Ye Z, Zhang L, Fang X, Zhang Z., Solar Energy Materials and Solar Cells, 136 (2015) 177–186.
[6] Vakili M, Hosseinalipour SM, Delfani S, Khosrojerdi S, Karami M., Solar Energy, 131 (2016) 119–130.
[7] Toppin-Hector A, Singh H., Int J Low-Carbon Tech, 11 (2016) 199–204.
[8] Wang N, Xu G, Li S, Zhang X., Energy Procedia, 105 (2017) 194–199.

# Numerical investigation of a directly irradiated solar rotary kiln for limestone calcination to maximize $CO_2$ flow and purity

Jana Barabas[1,2], Gkiokchan Moumin[1], Clarisse Lorreyte[1], Christian Sattler[1,2]

[1]*German Aerospace Center (DLR), Institute for Future Fuels*
[2]*RWTH Aachen University, Chair for Solar Fuel Production, Aachen, Germany*
*Jana.barabas@dlr.de*

The demand for cement has almost tripled in the last 25 years, and $CO_2$ emissions from cement production now account for 8% of global emissions from the industrial sector. One possibility to provide the required process heat is the use of centralized solar power. With the help of solar heat, the burning process in the calcination of limestone is to be replaced, thus reducing $CO_2$ emissions. Initial tests and the successful implementation of such a system have already been demonstrated at DLR [1].

One challenge in the development of such reactors is the deposition of particles on the glass at the reactor aperture. This leads on the one hand to overheating of the disk and on the other hand to less irradiation of the solar energy. Previous solutions to this problem range from indirectly irradiated cement reactors [2] to the use of cooling gases on the pane [3]. Nevertheless, the use of a glass pane reduces the incoming solar radiation. In addition, the upscaling of the glass also becomes a challenge due to the high temperatures involved. The commissioning of an open and directly irradiated solar reactor may be a possible solution. Previous studies using an open to ambient aperture have looked at a vortex reactor. By drawing air through the opening in a controlled manner a good thermal efficiency could be achieved and the leakage of particles through the opening could be reduced [4].

Since the system to be investigated operates under a $CO_2$ atmosphere due to the reaction process, the gas is to be extracted and therefore a mixing of $CO_2$ and air is to be avoided as far as possible. By controlling pressure and gas flow with different configurations at the reactor opening, the egress of particles and $CO_2$ leakage through the aperture should be prevented. In addition, the extracted $CO_2$ mass flow should be maximized while the inflowing air is minimized. In order to check the feasibility and efficiency of the system, a numerical flow field analysis is carried out to determine characteristic values such as the flow profile, the suction power as a function of the gas flow rate and the $CO_2$ leakage, as well as the mixing of gases.

[1] G. Moumin, S. Tescari, P. Sundarraj, L. de Oliveira, M. Roeb, C. Sattler, *Solar Energy* **182**, 480 (2019).
[2] A. Meier, E. Bonaldi, G.M. Cella, W. Lipinski, D. Wuillemin, *Solar Energy* **80**, 1355 (2006).
[3] E. Koepf, W. Villasmil, A. Meier, Author(s) 2016, p. 120005.
[4] A. Chinnici, D. Davis, T. Lau, D. Ang, M. Troiano, W.L. Saw, Z.F. Tian, R. Solimene, P. Salatino, G.J. Nathan, *Solar Energy* **231**, 185 (2022).

# High temperature aging of fluoro- and perfluororubber: Application in a receiver-reactor cavity system

Estefanía Vega Puga[1,2], Stefan Brendelberger[1], Christian Sattler[1,2]

[1] German Aerospace Center (DLR), Institute for Future Fuels
[2] RWTH Aachen, Chair for Solar Fuel Production
estefania.vegapuga@dlr.de

Solar thermochemical processes are promising technologies for cost effective, large-scale hydrogen and drop-in fuel production. Some of the most investigated thermochemical cycles utilize metal oxides (e.g. $CeO_2$) to split water and/or carbon dioxide in a two-step process, in which the high temperature (1500 °C) requirement is achieved by using concentrated solar radiation. Up to date, the most advanced system uses stationary monolithic redox structures and has a demonstrated efficiency of 4.1% at 50 $kW_{thermal}$ scale in field [1]. Recently, the R2Mx receiver-reactor concept has been proposed with the aim of increasing the solar-to-fuel efficiency [2].

This presentation will focus on the experimental demonstration of the aforementioned R2Mx receiver-reactor cavity system, where reliable and cyclic atmosphere separation between the two reaction zones has been identified as one of the main challenges, due to high temperatures and vacuum operation. Elastomers, namely fluororubber (FKM) and perfluororubber (FFKM), have been selected as sealing material in the form of O-rings. With ageing, elastomers can gradually lose their elasticity and their ability to recover, which might result in incremental leakage. An increase in leakage between the reactor zones can result in lower reactor efficiencies, as a lower reduction extent of the redox material is achieved and therefore less product fuel is produced at otherwise same operating conditions. Operability issues are also of interest, to quantify how often does the sealing need to be replaced and consider maintenance issues.

To assess the service lifetime of the pressure separation sealings, an accelerated ageing programme of FKM and FFKM O-rings at six different temperatures between 200°C and 375°C has been performed. O-rings are aged in compression by 25% for up to 14 days. Compression set measurements are used for characterising the seal performance while hardness measurements are utilised for retrieving information about the change of the seal's mechanical

properties. First results from the experimental campaign and correlations between pressure force, ageing and leakage rate are evaluated and presented.

## References

[1] S. Zoller S, E. Koepf, D. Nizamian, M. Stephan, A. Patané, P. Haueter, et al, Joule 6 (2022) 1606–1616.

[2] S. Brendelberger, P. Holzemer-Zerhusen, E. Vega Puga, M. Roeb, C. Sattler, Solar Energy 235 (2022) 118–128.

# Progress in modelling the thermal performance of a Linear Fresnel Collector with a Trapezoidal Cavity Multi-tube Receiver

Sergio Alcalde-Morales[1,2], Loreto Valenzuela[1], J.-J. Serrano-Aguilera[2]

[1]*CIEMAT-Plataforma Solar de Almería, Crta. Senes, km 4.5, 04200 (Almería), Spain;*

*e-mail: sergio.alcalde@psa.es*

[2]*Universidad de Málaga, Escuela de Ingenierías Industriales, Campus de Teatinos s/n, 29071, Málaga, Spain.*

### 1. Introduction

The aim of this thesis is to analyze Linear Fresnel solar Collectors (LFC) with cavity receivers using a multi-tube absorber. The focus is on an innovative LFC [1] that is currently being commissioned at the Plataforma Solar de Almería (PSA). Previous studies have implemented 3-D models, but with high computational cost [2-3]. As previously reported [4], a 3-D model was proposed with a 1-D heat transfer fluid (HTF) approach. This work takes a similar strategy, modeling LFC thermal behavior of the LFC by coupling the heat conduction in the absorber wall with the HTF domain. The main objective is to find an analytical solution to the 3-D heat equation under LFC specific operating conditions. Previous studies suggest that an analytical resolution may be faster than a numerical one. Therefore, the feasibility of such analytical solutions is investigated. Furthermore, a method is established to analyze heat losses in solar systems by taking into account the tube temperature, using an analytic solution applicable to cylinders with hollow structures in any facility.

### 2. Methodology

To solve this problem, heat loss correlations from a previous work are used. These correlations evaluate the heat losses from the absorber tubes as a function of their external temperature. The transient 3D heat equation is given by eq. (1), which is solved by applying separation of variables. If we let $T$ be $T(r, \theta, z, t) = h(t)i(z)g(\theta)f(r)$, four ODEs are obtained (eqs. (2), (3), (4) and (5)), whose solution gives the final solution of eq. (1).

$$\nabla^2 T = \frac{\rho C_p}{k}\frac{\partial T}{\partial t} \tag{1.a}$$

$$T(r, \theta, z, 0) = 300\,K; \ aT\big|_{r=r_1} + b\frac{\partial T}{\partial r}\big|_{r=r_1} = c; \ \frac{\partial T}{\partial r}\big|_{r=r_2} = q_{HTF} \tag{1.b}$$

$$\frac{dh}{dt} = -\frac{\lambda}{\sigma}h \tag{2}$$

$$\frac{d^2 i}{\partial z^2} = -\mu\, i \tag{3.a}$$

$$\frac{di}{\partial z}\Big|_{z=0} = \frac{di}{\partial z}\Big|_{z=L} = 0 \tag{3.b}$$

$$\frac{d^2 g}{d\theta^2} = -\xi\, g \tag{4.a}$$

$$g(0) = g(2\pi);\ \frac{dg}{d\theta}\Big|_{\theta=0} = \frac{dg}{d\theta}\Big|_{\theta=2\pi} \tag{4.b}$$

$$r\frac{d}{dr}\left(r\frac{df}{dr}\right) + \left((\lambda - \mu)r^2 - m^2\right)f = 0 \tag{5}$$

where boundary conditions are expressed for each ODE. $\sigma = \frac{\rho C_p}{k}$ is a constant that depends on the material, while, $\lambda, \mu$ and $\xi = m^2$ are the eigenvalues of each ODE, determined by the boundary conditions. The constants $a, b$ and $c$ in equation 5.b ¿DONDE ESTA LA ES 5B?must be recalculated at each iteration as they depend on the temperature. This is for linearising the correlations. $q_{HTF}$ represents the heat transfer from the tube to the heat transfer fluid. $L$ is the length of the pipe under consideration. It is important to note that eq. (5) is a Bessel equation whose solution is a linear combination of Bessel functions ($J$ and $Y$) of order $m$. The complete solution for T is given by eq. 6:

$$T(r,\theta,z,t) = \sum_{Sp=1}^{2}\sum_{m=1}^{\infty}\sum_{n=1}^{\infty}\sum_{j=1}^{\infty}(e^{-\frac{\lambda_{Sp,m,n,j}}{\sigma}t} \cdot \left(C1_{Sp,m,n,j}\cos(m\theta) + \right.$$
$$C2_{Sp,m,n,j}\sin(m\theta)) \cdot \cos\left(\frac{n\pi z}{L}\right) \cdot \left(C3_{Sp,m,n,j}\, J_{m,n}\left(m, \sqrt{\lambda_{Sp,m,n,j} - \mu_n} \cdot r\right) + \right. \tag{6}$$
$$\left. C4_{Sp,m,n,j}\, Y_{m,n}\left(m, \sqrt{\lambda_{Sp,m,n,j} - \mu_n} \cdot r\right))\right)\ .$$

$C1, C2, C3$ and $C4$ are constants that must be calculated by applying the boundary conditions and the initial conditions (eq. (1.b)) for each $m, n, j$ and for each subproblem $Sp$. Two subproblems with homogeneous boundary condition at $r = r_1$ and $r = r_2$ respectively must be solved in order to obtain $\lambda$ and the coefficients in each case. The solution is the sum of both. On the one hand, $m$ and $n$ are integers greater than 0 which determine the eigenvalues $\lambda$ and $\xi$ obtained by the boundary conditions 4.b and 3.b respectively. On the other hand, $j$ represents the zeros of the Bessel equation obtained from the homogenous boundary condition (1.b). The coefficients can be calculated by using the orthogonality property of the eigenfunctions of each ODE ($f, g, h, i$) [5]. The process was carried out as described in Özışık et al [6]. As expressed in the *Handbook of Mathematical Functions* [7], the $Y_m$ function is not an orthogonal function, so some simplifications have to be made to address the problem.

[1] Pulido D, Valenzuela L, Serrano JJ and Fernández A. Renew Energy 2019;131:1089-106.

[2] Cheng Z, He Y, Xiao J, Tao Y, Xu R. Int Commun Heat Mass Transfer 2010;37(7):782–7.

[3] Cheng Z, He Y, Cui F, Xu R, Tao Y. Sol Energy 2012;86(6):1770–84.

[4] Serrano-Aguilera JJ, Valenzuela L and Parras L. Applied Energy 2014;132:370-382.

[5] Haberman R. Applied Partial Differential Equations (4th Edition) Prentice Hall (2003).

[6] Hahn DW, Necati Özışık MN. Heat conduction. John Wiley & Sons (1993).

[7] Abramowithz M and Stegun IA. Handbook of Mathematical Functions (1964).

# DLR site in Köln-Porz



**Adress:**

**Deutsches Zentrum für Luft- und Raumfahrt (DLR)**
**Linder Höhe**
**51147 Cologne**

**Bus:** Line 162 to DLR

**Entrance:** Here you have to show your ID

**Lecture hall:** DLR Casino (Building 53)